INORGANIC CHEMISTRY

FRONTIERS

Accepted Manuscript

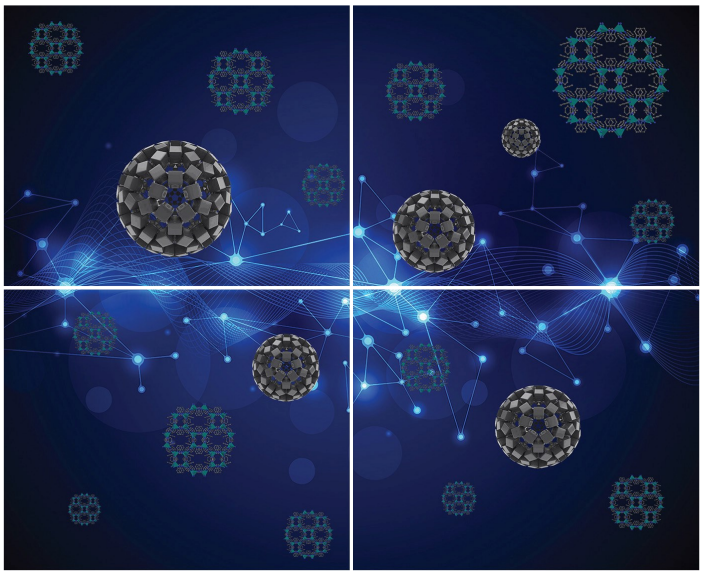

This article can be cited before page numbers have been issued, to do this please use: Q. Wang and G. Li, *Inorg. Chem. Front.*, 2020, DOI: 10.1039/D0QI01055C.

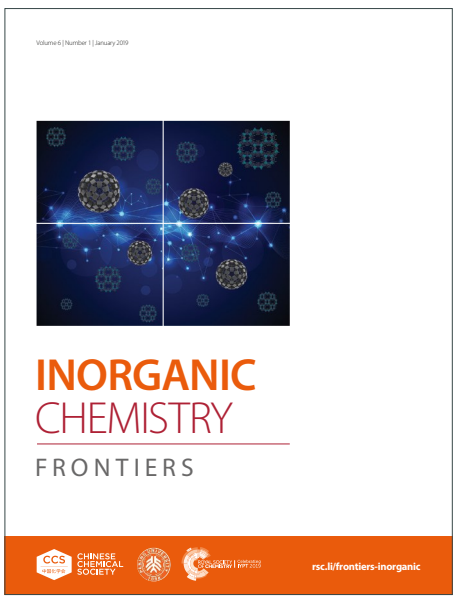

View Article Online
DOI: 10.1039/D0QI01055C

REVIEW

Bi(III) MOFs: Syntheses, structures and applications

Received 00th January 20xx,
Accepted 00th January 20xx

DOI: 10.1039/x0xx00000x

Qing-Xu Wang and Gang Li*

Metal-organic frameworks (MOFs) are favored by researchers on account of their high surface area, lofty porosity, excellent structural stability and diverse structures, and have been widely used in catalysis, sensing, adsorption, proton conduction, etc. Although the research of most MOFs has made amazing progress, the reports on Bi-based MOFs are limited. Nevertheless, because bismuth metal is non-toxic and environmentally friendly, and its radius is relatively large and has a high affinity for oxygen and nitrogen atoms, the Bi(III) MOFs with varied structure and various properties have attracted considerable attention recently. Additionally, owing to the structural advantages of Bi(III)-based MOFs, more and more interest has been aroused in the design and preparation of such MOFs, especially in the application research. Nevertheless, as far as we know, no review has concluded the latest research progress of these MOFs. We believe that a comprehensive review of the recent preparation, structures and properties of such MOFs would be very helpful for further research. Therefore, this review will summarize the preparation strategies, crystal structures and a variety of applications of bismuth-containing MOFs in the past ten years, and looks forward to the future.

1. Introduction

MOFs are crystalline porous materials that are constructed by metal ions/clusters and organic ligands. Compared to traditional porous materials like zeolite, they have quite a few advantages such as higher specific surface, higher porosity, adjustable pore size, and diverse structures.[1-4] Moreover, the most prominent advantage of MOFs is that their structures can be regulated and controlled during or after synthesis.[5] So far, MOFs have been widely used in catalysis,[6,7] fluorescence,[8-12] gas adsorption,[13-15] proton conduction,[16-20] sensors[21-24] and so on. In recent years, the research of MOFs has advanced rapidly, and thousands of MOFs have been synthesized. Due to its unique structural characteristics, there are many potential applications waiting for researchers to explore in depth.

Bismuth is a relatively rare heavy metal element (ranked 64th in abundance in the earth's crust). Unlike general toxic heavy metals, such as lead and mercury, it is safe and non-toxic. Researchers attribute its low toxicity to its low solubility and its inhibitory effect on bacteria.[25,26] So several bismuth compounds are the main ingredients in the treatment of gastric diseases, such as bismuth salicylate, colloidal bismuth citrate, and so on. Bismuth-based compounds have been adopted in pharmaceutical preparations for hundreds of years (since the eighteenth century).[27-29]

College of Chemistry, Zhengzhou University, Zhengzhou 450001, Henan, P. R. China. E-mail: gangli@zzu.edu.cn

The electronic configuration of bismuth atom is $[Xe]4f^{14}5d^{10}6s^26p^3$. Because of the weak shielding effect of 4f electrons (lanthanide shrinkage), Bi(III) compounds reveal Lewis acidity.[30,31] Under normal circumstances, bismuth is stable. During the coordination process, the three 6p electrons in the outermost layer are responsible for the formation of bonds, and bismuth usually exhibits +3 valence and has a high affinity for multidentate ligands containing oxygen and nitrogen atoms.[32] Additionally, bismuth metal also has catalytic activity, so bismuth complexes are often used as green catalysts. Because bismuth is non-toxic, harmless, has a larger atomic radius, a variety of coordination environments, and is relatively cheap, people began to turn their attention to the study of bismuth-based MOFs.[33,34] With increasing attention to environmental issues and green chemistry, people's interest in bismuth-based MOFs has greatly increased. The Bi-based MOFs have such advantages as various structures (from zero-dimensional to three-dimensional structures), high stability, easy preparation, and the potential value in the fields of photocatalysis, medicine, etc. Thus, more and more new bismuth-based MOFs have been synthesized. Herein, this review will summarize the latest progress of such MOFs and highlight their future applications. A summary of the Bi-MOFs that appeared in this review is shown in Table 1.

2. Synthesis methods of bismuth-based MOFs

2.1. Hydrothermal/solvothermal synthesis

Hydrothermal reaction is one of the most commonly used approaches for MOFs synthesis. Generally, metal salts, organic ligands and other substances that do not react or are difficult to react at room temperature are mixed uniformly in water, and then sealed in a Teflon-lined reactor for heating. Consequently, the reactor was kept at appropriate high temperature and appropriate high pressure for a period of time to make the reactants fully react, then cool down for growing single crystal products of the MOFs. The factors affecting the crystal growth mainly include reactant concentration, reactant proportion, stirring time, reaction time and so on. At present, this method is quite mature in the synthesis of bismuth MOFs. Note that because bismuth(III) is readily hydrolyzed, bismuth-containing oxides are usually substituted for bismuth salts for hydrothermal reactions. For example, in 2009, Tran et al. synthesized a 3D MOF **$Bi_2O_2(3,5\text{-}pdc)_2$** (denoted **ARL-3**) *via* hydrothermal reaction of $Bi(NO_3)_3{\cdot}5H_2O$ and 3,5-H_2pdc (3,5-pyridine-dicarboxylic acid) at a range of temperature(130, 165 and 200°C) for 72h.[35] It contains embedded 1D $[Bi_2O_2]^{2+}$ cationic chains, and has good thermal stability under 400 °C. In 2012, using Bi_2O_3 and $HO_3SC_2H_4SO_3H$ (1,2-ethanedisulfonate), a 3D MOF, **$Bi(O_3SC_2H_4SO_3)_{1.5}(H_2O)_2$** was hydrothermally prepared by Gschwind's group.[36] Its structure will be described in the latter part.

The principle of solvothermal synthesis and hydrothermal synthesis is similar, only the reaction solvent is different. In the solvothermal synthesis, other solvents, such as methanol (MeOH), ethanol (EtOH), acetonitrile, etc., can also be added in addition to water. Since most organic ligands are not extremely soluble in water, organic solvents are chosen to dissolve them. Importantly, organic solvents are sometimes involved in coordination, complicating the structures of the related MOFs. For, example, In 2014, Wang et al. described the first bismuth-based MOF, **Bi-mna** through the solvothermal reaction of bismuth nitrate with 2-mercaptonicotinic acid (H_2mna) and KOH in *N*, *N*-dimethylformamide (DMF) solution under 100 °C for 72 h.[37] In **Bi-mna**, the central bismuth atom is hexahedral and connected with four different organic ligands through sulfhydryl S, pyridine N and carboxyl O atoms. Two spiral channels are formed along *b*- and *c*-axes. The authors found that **Bi-mna** can decompose organic dyes RhB (Rhodamine B) and MB (Methylene blue) under visible light irradiation.

Note that the routine solution synthesis method is also commonly adopted in the preparation of Bi-based MOFs. The essence of this method is to mix the metal salt, organic ligands and solvent evenly, diffusing at room temperature, thus slowly growing the crystal at the phase interface. It has the advantages of mild reaction conditions and easy to obtain high-quality crystals. For example, two MOFs **2 $\infty[Bi(ADC)_{2/4}(ADC)_{3/3}(H_2O)_2]{\cdot}2H_2O$** (**Bi-ADC-01**) and **3 $\infty[Bi(ADC)_{2/4}(ADC)_{3/3}(H_2O)_3]{\cdot}H_2O$** (**Bi-ADC-02**) were obtained through evaporation of $Bi(NO_3)_3{\cdot}5H_2O$ and acetylenedicarboxylic acid (H_2ADC) in H_2O at room temperature by Busch et al. in 2012.[38] Also， Roodsari et al. reported a MOF, **[Bi(pcih)(μ-ONO_2)$(NO_3)_2CH_3OH$]** through the branch tube method.[39] They used MeOH to dissolve $Bi(NO_3)_3{\cdot}5H_2O$ and 2-pyridinecarbaldehyde isonicotinoylhy-drazone (Hpcih) ligand in the two arms of the branch tube and sealed the tube. The branch arm containing the ligand was heated at 60 °C, and the other branch arm was placed at room temperature. A few days later, a single crystal was obtained in the arm at 25 °C.

2.2. Microwave synthesis

The microwave synthesis applies microwave technology to make the chemicals inside the heated body perform high-frequency reciprocating motion.[40-42] Unlike traditional heating, it has uniform heating, high efficiency and low energy consumption. In 2012, a porous and catalytically active material **Bi(BTB)** was successfully prepared by M. Feyand et al. by either solvothermal synthesis or microwave synthesis.[41] The solvohermal reaction is performed in MeOH at 120 °C for 12 hours. In contrast, the mixture of bismuth(III) nitrate pentahydrate, 1,3,5-benzenetrisbenzoate (H_3BTB) and CH_3OH was sealed in a microwave reactor and exposed it to 120°C

Qing-Xu Wang

Qing-Xu, Wang obtained his B. Eng. degree in College of Chemistry and Chemical Engineering from Shanxi University in 2017. He is currently a M. Eng. student under the supervision of Professor Gang Li in Zhengzhou University. He works on the design and synthesis of functional MOFs for exploring their applications in proton conduction.

Gang Li

Gang Li received his B.S. degree and M.S. degree in inorganic chemistry from Zhengzhou University, China. He obtained his Ph. D degree in 2003 in Shanxi University, China. Then he joined the Zhengzhou University. From January to July in 2004, he worked at Chinese University of HongKong as a Visiting-Scholar. Then, he worked as a postdoctoral fellow at University of Sussex from September, 2004 to September, 2005 under the supervision of Professor M. F. Lappert. He became a professor in Chemistry at the Zhengzhou University in 2008. Li Group's research interests are centered on the design of various functional solid crystalline materials (MOFs, COFs and HOFs) to develop their applications in the field of energy and identification.

microwave oven for 20 minutes to produce the product. Obviously, the difference between the two is that the reaction time is greatly shortened in microwave synthesis.

2.3. Other synthetic methods

In addition to the above several widely used synthetic methods, other methods have recently emerged, such as mechanochemical synthesis,[43] heating reflux method,[44,45] sonochemical synthesis and so on.[46,47]

Mechanochemical method refers to the use of mechanical external forces (such as extrusion, grinding, shearing, etc.) under the condition of less or no organic solvents to apply mechanical energy to the reactants, thereby inducing changes in their physical properties and chemical reaction, which is a rapid, efficient, and solvent free method. In 2014, Two Bi-MOFs, **$(H_2Im)[Bi(1,4\text{-}bdc)_2]$** and **$[Bi(2,5\text{-}pdc)(NO_3)_2(H_2O)_2]\cdot H_2O$** (Him = imidazole; 1,4-H_2bdc = 1,4-benzenedicarboxylic acid; 2,5-H_2pdc = 2,5-pyridinedicarboxylic acid) were successfully obtained through mechanochemical (grinding) method by Emmerling group.[43] Heating reflux method usually refers to the process under atmospheric pressure, oil bath heating reflux, speeds up the reaction process, the formation of products. For instance, in 2020, IRAM et al. successfully synthesized bismuth complex **$[Bi(bda)_3]_n$** by means of heated reflux the mixture of bismuth nitrate, biphenyl-4,4′-dicarboxylic acid (H_2bda) and DMF.[44] The fluorescence and gas adsorption of the MOF were studied. In 2019, a new Bi-MOF, **[Bi(HBTC)(Ac)]** (H_3BTC = 1,3,5-benzenetricarboxylic acid) was obtained by using acetic acid (HAc) as solvent by means of reflux method.[45] Sonochemical synthesis is similar to microwave synthesis.

3. Structures of Bi(III) MOFs

3.1. MOFs constructed with phenyl ligands

Usually, organic ligands act as the key role in the preparation of Bi-MOFs, which can directly affect the structures and performance of subsequent products. Therefore, in this review, we mainly describe the related MOFs in the light of the main skeleton classification of the organic compounds adopted. The schematic diagrams of these organic phenyl ligands adopted are shown in Scheme 1.

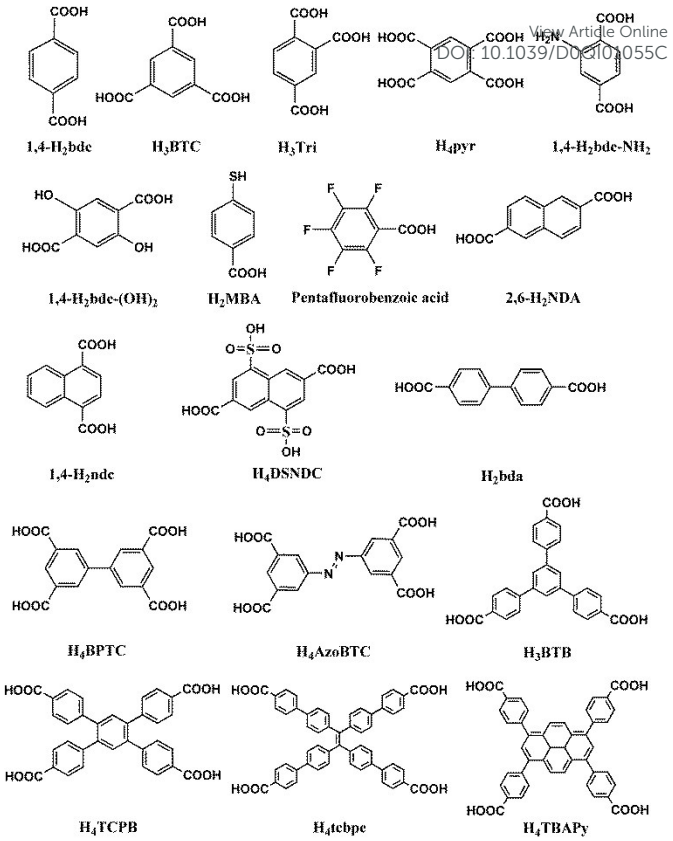

Scheme 1 Schematic of the chemical structures of benzene ring ligands mentioned in this review.

Four Bi-MOFs, **$[Bi(1,4\text{-}bdc)_2(DMF)]\cdot(Hdma)\cdot 2DMF$** (**A1**), **$[Bi(1,4\text{-}bdc)_2]\cdot(Hdma)\cdot DMF$** (**A2**), **$[Bi_4(1,4\text{-}bdc)_7(HIm)]\cdot 2(Hdma)\cdot 2DMF$** (**A3**) and **$[Bi(1,4\text{-}bdc)_2]\cdot(Hdma)$** (**A4**) (Hdma = dimethylammonium cation) have been solvothermally prepared and characterized by Thirumurugan et al. in 2020.[48] Except **A1** is a two-dimensional structure, the others are three-dimensional frameworks. The four MOFs contain anionic frameworks and Hdma cations. In **A1**, the Bi^{3+} is bound to nine O atoms. Each Bi^{3+} is linked to four other Bi^{3+} atoms by the 1,4-bdc^{2-} ligands resulting in a layer structure. In **A2**, the Bi^{3+} is eightfold coordinated by O atoms from four distinct 1,4-bdc^{2-} anions. The Bi^{3+} atoms are joined by 1,4-bdc^{2-} anions to make up a 3D network. Different from **A1** and **A2**, in **A3**, there are two kinds of Bi^{3+} cations: Bi(1) and Bi(2), which are both nine-coordinated. Bi(1)NO_8 and Bi(2)O_9 are linked to a dimer through three carboxyl groups. These dimers are joined through 1,4-bdc^{2-} anions to build up a 3D structure. Similar to **A3**, **A4** also contains two types of Bi^{3+}: Bi(3) and Bi(4). Bi(3) is nine-coordinated locating in a Bi(3)O_9 polyhedron. Bi(4) is twelvefold-coordinated siting in a Bi(4)O_{12} polyhedron. The Bi(III) atoms are joined by the organic ligands to constitute a 3D structure.

Earlier, a novel 3D Bi-MOF, **$(H_2Im)[Bi(1,4\text{-}bdc)_2]$** was synthesized through mechanochemical by Emmerling group.[43] In this MOF, there are two kinds of coordination environments

for Bi^{3+} ions. Bi1 is twelve-coordinated and Bi2 is nine-coordinated. The connection between the 1,4-bdc^{2-} and the bismuth polyhedron leads to a three-dimensional framework.

Burrows et al. successfully solvothermally synthesized four MOFs, **$[Bi_2(1,4\text{-}bdc)_2(dfp)_2]\cdot DMF$** (**B1**), **$[Bi_2(1,4\text{-}bdc)(dfp)_4(H_2O)_2]\cdot 2DMF$** (**B2**), **$[Bi_2(1,4\text{-}bdc\text{-}NH_2)(dfp)_4(H_2O)_2]\cdot 2DMF$** (**B3**) and **$[Bi_2\{1,4\text{-}bdc\text{-}(OH)_2\}(dfp)_4(H_2O)_2]\cdot 2DMF$** (**B4**), employing 1,4-H_2bdc, 2-amino-1,4-benzenedicarboxylic acid (1,4-bdc-NH_2), 2,5-dihydroxy-1,4-benzenedicarboxylic acid (1,4-bdc-$(OH)_2$) and deferiprone (Hdfp).[49] In **B1**, each nine-coordinated bismuth center is connected by 1,4-bdc^{2-} ligands to build up a chain with dfp hanging on this chain. The MOFs **B2**, **B3** and **B4** are isostructural. In **B2**, the central bismuth atom was coordinated by a bidentate carboxylate group and two bidentate dfp ligands to form six Bi-O bonds. Additionally, there are two long Bi-O bonds in the bismuth center, one is connected to water molecules, and the other is connected to carboxylic acid groups to form a dimer.

Nguyen et al. prepared a MOF, **Bi-bdc**, by means of solvent heat and microwave-assisted heating using 1,4-H_2bdc ligand lately.[50] In the former method, bismuth nitrate and 1, 4-H_2bdc were dissolved in DMF (molar ratio M: L = 1:1.5) and stirred. Subsequently, the mixture was put into a vessel, heated to 120 °C, and kelp for 2 days to obtain **Bi-bdc-ST**. Microwave method can be used to reduce the reaction time. After the above reactants are mixed thoroughly, they are put into the microwave heating reactor and heated by pre-programmed heating method (reaction temperature: 120°C; Time: 60 min; the power: 400W). After the reaction, post-processing was carried out to get **Bi-bdc-MW**.

Feyand and coworkers reported eight MOFs, **$Bi_2(O)(Pyr)(H_2O)$ (C1)**, **Bi(HPyr) (C2)**, **Bi(HPyr) (C3)**, **Bi(Tri)(H_2O) (C4)**, **Bi(Tri) (C5)**, **$[(Bi(BTC)(H_2O)]\cdot H_2O$ (C6)**, **$Bi_6O_5(BTC)_2(HBTC)$ (C7)**, **$Bi_2(O)(OH)(HBTC)(NO_3)$** (**C8**), employing three organic ligands, 1,2,4,5-benzenetetracarboxylic acid (H_4Pyr), 1,2,4-benzenetricarboxylic acid (H_3Tri) and H_3BTC, *via* High-throughput methods.[51] In **C1**, eight-coordinated Bi(III) atoms have two kinds of coordination environments. The formation of Bi_4O_{12} units is caused by O^{2-} ions coplanar with the BiO_8 polyhedron. In **C2**, the corner BiO_9 polyhedron is attached to the zigzag chain. The Bi-O chains were linked by aromatic rings of the organic ligands to construct a 3D framework. In **C3**, the coordination surrounding the Bi, edge-sharing of BiO_9 polyhedron leads to the formation of Bi-O-chains. These Bi-O chains are connected by ligands. In **C4**, the coordination environment of Bi^{3+} ion is composed of 7 carboxylic O atoms and one water unit. The edge sharing of the BiO_8 polyhedron leads to chain formation. The crystal structure of **C5** is not obtained. The asymmetric unit of **C6** has one Bi^{3+} ion, one BTC^{3-} ion, one coordination H_2O and one free H_2O. The central Bi^{3+} ion is eightfold coordinated. Edge-sharing of two BiO_8 polyhedra results in Bi_2O_{14} dimers. The dimers through the benzene ring along b-axis lead to a 3D network. In **C7**, Bi^{3+} ions are 7-coordinated or 9-coordinated. They are surrounded by oxygen atoms from carboxylic acids and O^{2-} ions. The Bi_6O_{31} units are attached to the chain along the a-axis. In **C8**, the Bi^{3+} ions form polyhedra for BiO_6 and BiO_8 and are connected with zig-zag double chains. These chains were interconnected by nitrate ions to build up a 2D sheet in the a,c-plane, which is joined by the ligands to form a three-dimensional network.

In 2018, a 1D Bi-MOF, **$[Bi(Pyr)_{0.5}(2,2'\text{-}bipy)(NO_3)(DMF)]$** (2,2'-bipy= 2,2'-bipyridine), was solvothermally prepared by Gomez et al.[52] Each Pyr ligand in this MOF adopts a bidentate chelation mode with four Bi centers to form a chain along the [100] direction, and the distance between adjacent Bi atoms is 6.3594(6) and 9.3852(7) Å, which are linked by weak H-bonds to make up a 3D supramolecular structure.

Wang et al. solvothermally synthesized a 3D Bi-MOF, **$[(Bi(BTC)(DMF)]\cdot DMF\cdot 2CH_3OH$** by using H_3BTC ligand,[53] in which the two Bi atoms form a $\{Bi_2O_{14}\}$ dimer with six carboxyl groups from six different BTC^{3-}, and the dimers are interconnected with the organic ligands to form a 3D structure. There are two types of 1D helix chains (Fig. 1a, 1b) Both two chains have right-handed and left-handed helix chains. As shown in Fig. 1c, the two helix chains share the same set of units (Fig. 1d).

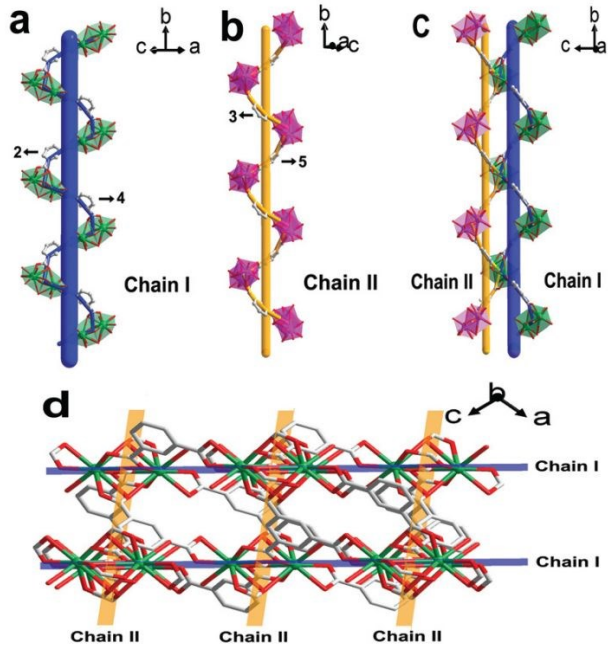

Fig. 1 1D helix chains (a) chain I, (b) chain II and (c) the two chains share the same set of units; (d) the assembly of chains I and II with an angle of 96.915°. Bi: green in (a, c and d); purple in (b, c); C: light grey; O: red, chain I: blue; chain II: yellow. Reproduced with permission from ref. 53. Copyright 2015, The Royal Society of Chemistry.

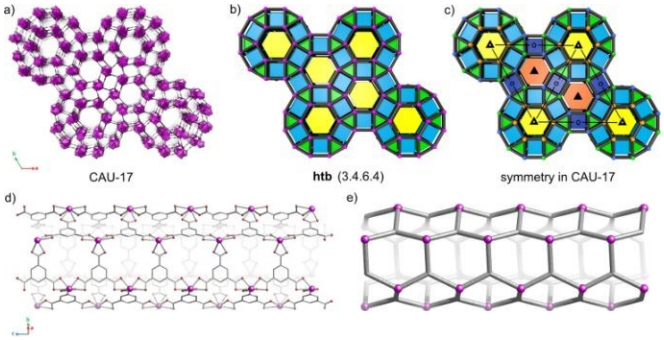

Fig. 2 Crystal structure of **CAU-17**. Reproduced with permission from ref. 40. Copyright 2016, American Chemical Society.

Inge group reported a porous 3D MOF, **[Bi(BTC)(H$_2$O)]·2H$_2$O·CH$_3$OH** {**CAU-17**, CAU (Christian-Albrechts-Universität)} with unprecedented topological complexity by means of microwave synthesis.[40] In this MOF, a great number of framework units exist in the asymmetric unit {9 Bi(III) cations, 9 BTC^{3-} anions and 9 coordination H$_2$O units}. Each nine-coordinated Bi(III) atom is bound to eight O atoms form the BTC^{3-} ligands and one O atom form a coordinated H$_2$O, and shares four O atoms with two adjacent Bi(III) atoms forming the spiral rods. These rods are joined by BTC^{3-} anions to form an intricate 3D framework (Fig. 2). The spiral chain, pore distribution, periodic network and topological structure in the MOF are analyzed and discussed in detail. Obviously, this is a typical example of a complicated structure constructed from simple building blocks, which deserves further study.

Consequently, Köppen group conducted more attempts on the synthesis of **CAU-17** in 2018, and the results showed that **CAU-17** was not only rapidly generated, but also further transformed into a dense phase with the extension of the reaction time.[54] With the increase of reactant concentration, **CAU-17** can be transformed another MOF, **Bi(HBTC)(NO$_3$)(CH$_3$OH)·CH$_3$OH**.

Ye and coworkers hydrothermally prepared another 3D MOF, **{[Bi(BTC)(H$_2$O)$_2$]·H$_2$O}$_n$**.[56] The central Bi is bound to nine O atoms, both of them from the coordination water and the others from four BTC^{3-} anions, forming a distorted mono-capped square antiprism. Three Bi(III) ions and BTC^{3-} anion are linked into a ring with size of 7.95 × 9.89 Å.

A new Bi-MOF, **[Bi(BTC)(H$_2$O)]·H$_2$O** was prepared through hydrothermal synthesis, and doped it with Eu^{3+}.[58] This MOF contains a dimer {Bi$_2$O$_{18}$}, which is connected with each other through BTC^{3-} anions to form a 3D framework with two kinds of channels having dimensions of 12.449 × 8.553 Å and 7.970 × 8.838 Å.

Savage group solvothermally prepared a MOF, **[Bi$_2$(BPTC)$_{1.5}$(H$_2$O)$_2$]·3.5DMF·3H$_2$O** (**NOTT-220-solv**) by employing biphenyl-3,3',5,5'-tetracarboxylic acid (H$_4$BPTC).[60] It exhibits a neutral and non-interpenetrated framework built by binuclear {Bi$_2$} cores and tetracarboxylate units. Note that this reaction results in two similar structures (namely α and β phases), except that the coordination environment of the central bismuth atom is slightly different. **NOTT-220-solv** is a highly porous structure bearing three distinct interconnected channels through binding of the ligands to the {Bi$_2$} nodes.

In 2016, Deibert team used 4', 4''', 4''' '', 4'''' ''''-(ethene-1, 1, 2, 2-tetrayl) tetrakis [(1,1'-biphenyl)-4-carboxylic acid] (H$_4$tcbpe) to solvothermally synthesize a 3D MOF **K[Bi(tcbpe)(DMF)$_2$]·xDMF** (**LMOF-401**).[61] The central Bi is bound to four carboxyl groups of four tcbpe ligands, and DMF also participates in the coordination. The K$^+$ forms a one-dimensional helical chain connecting the Bi-tcbpe networks by carboxyl oxygen and solvent oxygen.

In the same year, a fluorine-containing 2D MOF, **[Bi(OOCC$_6$F$_5$)$_3$(2,2'-bipy)(H$_2$O)$_2$]**(**Bi-FMOFs**) was presented by Kong et al. using C$_6$F$_5$COOH (pentafluorobenzoic acid) ligand.[62] In its structure, the central nine-coordinated Bi(III) sited in a polyhedral BiN$_2$O$_7$, in which two N atoms are from 2,2'-bipy, six oxygens come from the carboxyl groups of three C$_6$F$_5$COO$^-$ ligands and one water molecule.

Stock's group successfully prepared six Bi MOFs, **[Bi$_6$O$_6$(OH)$_2$(H$_2$O)$_4$(DSNDC)]** (**D1**), **[Bi$_2$(OH)$_2$(DSNDC)]** (**D2**), **[Bi$_8$O$_7$(OH)$_2$(H$_2$O)$_2$(DSNDC)$_2$]** (**D3**), **[Bi$_7$O$_5$(OH)$_3$(H$_2$O)$_4$(DSNDC)$_2$]·4H$_2$O** (**D4**), **[Bi$_2$(OH)$_2$(H$_2$O)$_2$(DSNDC)(H$_2$DSNDC)]** (**D5**), **[Bi$_6$O$_4$(OH)$_4$(H$_2$O)$_{12}$(H$_2$DSNDC)$_3$]·xH$_2$O** (**D6**) with 4,8-disulfonyl-2,6-naphthalenedicarboxylic acid (H$_4$DSNDC) in 2018 through high-throughput methods.[63] In situ PXRD of synchrotron radiation was used to investigate the reaction conditions. In **D1**, Bi^{3+} ions are seven (Bi1) or eight (Bi2, Bi3) coordinated. The Bi-O polyhedra are linked by edges and surfaces to consitute infinite iD Inorganic building units (IBUs). Each carboxylate and sulfonate unit coordinates to a single Bi^{3+} ion (Bi2) from four different IBUs, allowing each IBUs to connect to the other eight IBUs to construct a dense 3D CP. In **D2**, each ligand is connected to eight Bi^{3+} ions, both of which are chelated with carboxyl, and three of which are bonded by each sulfonic acid group. These dimeric units are shared by the edges in the cambium in the ab plane. The naphthalene ring is connected to two-dimensional IBU to form dense three-dimensional CP. In **D3**, a {Bi$_{16}$O$_{14}$(OH)$_4$} cluster is formed, and a one-dimensional IBUs is formed along a-axis by combining two water molecules with the other two clusters. In **D4**, Bi1, Bi3 and Bi4 are coordinated by eight oxygen atoms, and Bi2 and Bi5 are coordinated by 10 and 11, respectively. O^{2-} and OH$^-$ ions bridge seven Bi^{3+} cations. Each of the IBUs is bound to eight ligands and is connected to the other 12 IBUs through them. In **D5**, Bi^{3+} ions coordinate with an oxygen atom of a H$_2$O, an OH$^-$, a chelating carboxylic acid group, and four different sulfonic acid groups. Each sulfonic acid group connects two Bi^{3+} ions along the a-axis to a chain. Naphthalene rings connect each of these chains to the other six chains to construct a 3D framework with 1D channels. In **D6**, the {Bi$_6$O$_4$(OH)$_4$} clusters can be formed.

In 2018, Köppen et al. reported three MOFs, **[Bi$_2$(H$_2$TCPB)(TCPB)(H$_2$O)$_2$]·xH$_2$O** (**CAU-31**),

(Hdma)[Bi(TCPB)(H_2O)]·xH_2O (**CAU-32**) and **[$Bi_4(O)_2(OH)_2$(H_2TCPB)(TCPB)(H_2O)$_2$]·xH_2O** (**CAU-33**) using $Bi(NO_3)_3·5H_2O$ and 1,2,4,5-tertrakis-(4-carboxyphenyl)benzene (H_4TCPB).[64] Note that the three MOFs were prepared by the same starting material but under different solvent conditions (MeOH, MeOH /DMF and DMF/toluene for **CAU-31**, **CAU-32** and **CAU-33**, respectively), which denotes that the solvent effect is prominent in this reaction system. **CAU-31** contains three Bi^{3+} ions chelated by three carboxylic acids forming a sheet. These 2D sheets show inclined interpenetration, building up a rare 3D interlocking structure (Fig. 3a). **CAU-32** is a three-dimensional skeleton structure of negative ions constructed by Bi^{3+} ions chelated with four carboxyl units and one water unit, showing a three-dimensional channel system (Fig. 3b). The IBUs of **CAU-33** is a bismuth oxide bar extending along c-axis. The bar is joined by H_2TCPB^{2-} and $TCPB^{4-}$ ions to build up a three-dimensional framework (Fig. 3c). Two 1D diamond channels parallel to the rod along the c-axis are formed, with diameters of 9.5 × 4.6 and 4.4 × 4.1 Å, respectively.

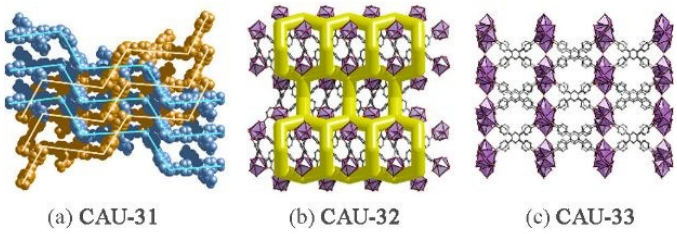

Fig. 3 (a) Inclined interlocking of layers in **CAU-31**. (b) The 3D channel system of **CAU-32**. (c) Crystal structure of **CAU-33**. Reproduced with permission from ref. 64. Copyright 2018, American Chemical Society

A novel Bi-MOF, **[(Hdma)Bi(1,4-ndc)$_2$(DMF)]$_n$·nDMF** (**E1**) was solvothermally synthesized by Lu et al. by adopting 1,4-H_2ndc (1,4-naphthalenedicarboxylic acid).[65] Each 1,4-ndc^{2-} ligand is connected to the Bi^{3+} ion in μ_2 coordination to form a layer. These layers can be constructed a 3D supramolecular structure across hydrogen bonds. The solvent DMF and Hdma cations are present in the voids.

In 2019, Vilela et al. reported a high-proton conductive Bi-MOF, **[Bi_4(HAzoBTC)$_2$(AzoBTC)(OH)$_2$(H_2O)$_4$]·7H_2O** (**IEF-2**).[66] **IEF-2** was hydrothermally synthesized by using a multi-carboxyl ligand 3,3′,5,5′-azobenzenetetracarboxylic acid (H_4AzoBTC). Free carboxyl groups exist in the structure, and hydrogen bonds are formed between free water and free carboxyl groups. In addition, other carboxyl groups and water molecules also form a large number of H-bonds, which establishes the structural basis for proton conduction.

Xiao group solvothermally synthesized a new 3D Bi-MOFs, **Bi-TBAPy** by employing 1,3,6,8-tetrakis(p-benzoic acid)pyrene (H_4TBAPy) ligand in 2019.[70] In this MOF, the central Bi atom coordinates with eight O atoms of the organic ligands. A Hdma coordinates with Bi atoms as a counter ion to maintain charge balance. Along the *a*-axis, there is a rhombus and a quadrilateral channel. Each $TBAPy^{4-}$ is connected with four Bi to form a three-dimensional structure.

In 2019, Guan and coworkers made another 3D structure, **Bi(TBAPy)**, by solvothermal synthesis,[71] in which the central Bi is coordinated with eight oxygen from four $TBAPy^{4-}$ ligands, forming a BiO_8 double-cap triangular prism. The four BiO_8 centers shared the organic ligand cambium and were joined to construct a 3D framework through the ligand $TBAPY^{4-}$. Along the *b*-axis there is a large channel of about 16.3 × 11.6 Å.

As described early, Feyand et al. found that in the preparation of **Bi(BTB)** (**CAU-7**),[41] the microwave method could shorten the reaction time and the addition of DMF was conducive to the growth of large rod-like crystals. The center Bi is allocated to create a BiO_9 threefold capped trigonal prisms. BTB^{3-} connects chains along the c direction to a slightly twisted cellular network with a 1D channel about 1 nm. The results of TG and TD-XRPD showed that **CAU-7** remained stable under 380 °C.

In this part, by describing the structures of Bi-MOFs constructed with phenyl ligands, we discovered that all ligands contain carboxylate groups, and most of the central bismuth atoms coordinate with carboxyl oxygen to form novel, complex multi-dimensional structures.

3.2. MOFs constructed by heterocyclic ligands

In addition to the benzene-containing ligands mentioned above, heterocyclic ligands were also employed and displayed strong coordination ability and various coordination modes. Their chemical structures are denoted in Scheme 2.

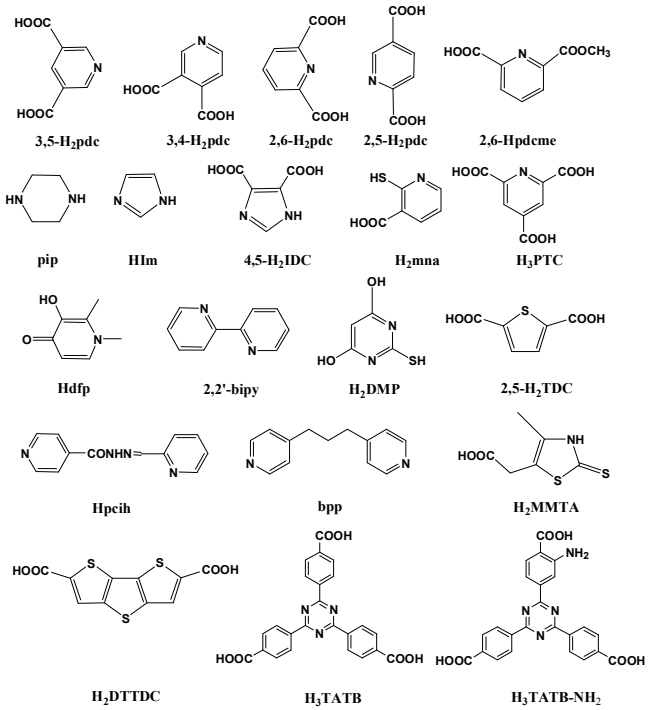

Scheme 2 The chemical structures of heterocyclic ligands mentioned in this review.

Pyridine dicarboxylic acid ligands are good building blocks and are commonly used in the preparation of Bi(III) MOFs. Wibowo group hydrothermally prepared a 2D MOF, **$Bi_3(\mu_3\text{-}O)_2(2,5\text{-}pdc)_2(2,5\text{-}Hpdc)(H_2O)_2$** in 2010.[74] The asymmetric unit includes three Bi^{3+}, two μ_3-O ligands, three dicarboxylate ligands, and one coordinated and one uncoordinated H_2O units. The Bi_6O_4 clusters are connected by organic ligands to construct a sheet. Moreover, these layers are joined through H-bonds to form a 3D supramolecular structure.

Lately, three MOFs, **Bi(2,5-pdc)(2,5-Hpdc)(H_2O)** (**F1**), **$K_4Bi(2,5\text{-}pdc)_3(2,5\text{-}Hpdc)(H_2O)_{3.3}$** (**F2**), and **$(Hdma)_3Bi(2,5\text{-}pdc)_2(2,5\text{-}Hpdc)_2$** (**F3**) were hydrothermally/ solvothermally prepared by Wibowo et al. [75] In **F1**, a zigzag chain is formed by connecting the central bismuth with the surrounding ligands, which is then bridged by H-bonds to constitute a 3D structure. As for **F2**, it is an interesting anion layer structure and is the first example of Bi-based clusters fabricating an anionic sheet of $[Bi(2,5\text{-}pdc^{2-})_3(2,5\text{-}Hpdc^{-})]^{4-}$ with counter ions locating in the interlayers. **F3** is a supramolecular molecule. In the asymmetric element of **F3**, including one anionic bismuth complex, $[Bi(2,5\text{-}pdc)_2(2,5\text{-}Hpdc)_2]^{3-}$, and three dimethylammonium cations. The anionic bismuth units, $[Bi(2,5\text{-}pdc)_2(2,5\text{-}Hpdc)_2]^{3-}$ balanced by three Hdma cations are formed 1D chains that extend along a-axis by H-bonds between O(3A)-H(3A)---O(16) from the mono-protonated ligand. Followed by using 2,5-H_2pdc, they reported another 2D MOF, **$Bi(2,5\text{-}pdc)_2(H_3O^+)(H_2O)_{0.83}$**.[76] The asymmetric unit contains a bismuth ion, one 2,5-pdc^{2-} ligand and some solvent molecules. The coordination sphere of BiO_6N_2 is completed by O and N atoms from the four 2,5-pdc^{2-} creating a slightly distorted double-hat octahedron. The layered structure formed by four 2,5-pdc^{2-} ligands and the central atom Bi, extending in the a-, b-direction of the crystal, and resulting in six-membered and three-membered rings with an overall arrangement related to the Kagomé topology.

After one year, the same group reported a 3D MOF, **$Bi_2O_2(2,5\text{-}pdc)$**.[77] It is the first polar, non-centrosymmetric 3D MOF with asymmetric ligands. The MOF includes Bi_2O_2 chains that are linked into a 3D framework *via* the 2,5-pdc^{2-} anions. On the Bi_2O_2 chains, the central Bi cations exhibit several kinds of coordination surroundings, $Bi(1)O_5N$, $Bi(2)O_6$, $Bi(1)O_5N$ and $Bi(2)O_6$.

Emmerling's group used 2,5-H_2pdc to obtain a 1D Bi MOF, **$[Bi(2,5\text{-}pdc)(NO_3)_2(H_2O)_2]\cdot H_2O$**.[43] The asymmetric unit contains one Bi^{3+} atom, one 2,5-pdc^{2-} unit, two nitrate anions and three H_2O units. The central Bi^{3+} ion is nine-fold coordinated forming a BiO_8N polyhedron. The monodentate coordination anion nitrate connects the complex to the adjacent Bi^{3+} cation, forming a one-dimensional chain of Bi^{3+} cation.

Thirumurugan group solvothermally synthesized six MOFs, **$[Bi(2,6\text{-}pdc)_3]\cdot 3(Hdma)$** (**G1**), **$[Bi(2,6\text{-}pdc)_3]\cdot 3(Hdma)\cdot 2H_2O$** (**G2**), **$[Bi(2,6\text{-}pdc)_2(DMF)]\cdot(Hdma)$** (**G3**), **Bi(2,6-pdc)(2,6-pdcme)(CH_3OH)** (**G4**), **$[LiBi(2,6\text{-}pdc)_3(H_2O)]\cdot 2(Hdma)$** (**G5**), and **$Li_5Bi(2,6\text{-}pdc)_4(H_2O)_2$** (**G6**) (2,6-$H_2$pdc =2,6-pyridinedicarboxylic acid; 2,6-Hpdcme = 6-methyl-oxycarbonyl pyridine 2-carboxylate) by varying the ratio of metal salt to ligand, [78] the type of solvent and different acid-base conditions. In **G1**, the infinite 2D H-bonding sheets are stacked involving π-π interactions between neighbor pyridine units. In **G2**, each Bi(III) atom is joined to four Hdma cations and two Hdma dimers to build up a H-bonded layer. In **G3**, there are two 2,6-pdc anions (-1 and -2). The two 2,6-pdc anions are tridentate chelated with a Bi^{3+} cation by the carboxylic acid group and the pyridine nitrogen. The 2,6-$Hpdc^-$ anion is also monodentate with another Bi^{3+} across the carboxylic acid to form a dimeric $[Bi_2(2,6\text{-}pdc)_4(DMF)_2]^{2-}$ anion. In **G4**, 2,6-pdcme monoanion was synthesized from 2,6-H_2pdc and methanol in situ. The coordination sphere around the central bismuth cation is BiN_2O_6. The 2,6-pdc^{2-}, 2,6-pdcme cations and Bi^{3+} cations are connected by monodentate or tridentate manner to form a neutral dimer with eight unmatched carboxylic oxygens. For **G5**, it is a 1D bimetallic compound. The bismuth unit was bridged by two Li^+ cations through two 2,6-$Hpdc^-$ anions to build up a chain with $Bi(2,6\text{-}pdc)_3$ unit and Li^+ ions alternately arranged. Two such parallel chains are linked to a lithium tetrahedron from one chain to the other via the 2,6-pdc^{2-} anion, thus forming a stepped one-dimensional chain structure. For **G6**, it's a 3D bimetallic compound. The Bi^{3+} atom is nine-coordinated by six O atoms and three N atoms of three organic ligands.

Consequently, Sushrutha and coworkers reported three MOFs, **$[pip][Bi(2,6\text{-}Hpdc)(2,6\text{-}pdc)]\cdot H_2O$** (**H1**), **[Bi(HIDC)IDC)]** (**H2**) and **$[Bi(\mu_2\text{-}OH)(3,4\text{-}pdc)]$** (**H3**) (pip = piperazine; 4,5-H_2IDC = 4,5-Imidazole dicarboxylic acid; 3,4-H_2pdc = 3,4-pyridinedicarboxylic acid).[79] In **H1**, carboxyl free oxygen can interact weakly with adjacent bismuth ions to form a chain structure through 2,6-$Hpdc^-$ ligands. In **H2**, The central Bi^{3+} ion is eight coordinated, which forms BiO_6N_2 distorted bicapped-trigonal prismatic geometry. The bismuth centers form a Bi_2O_2 dimer through the μ_3-O, which produces the bilayer arrangement. The asymmetric unit of **H3** is composed of one Bi^{3+}, one 3,4-pdc and one μ_2-hydroxyl. The Bi centers are linked by μ_2-hydroxyl O atoms to form Bi_2O_2 dimeric units. The dimes are bridged by carboxylic acid groups to fabricate a 3D structure through the connection of pyridine nitrogen and other carboxylic acid groups.

Huang et al. successfully synthesized a 1D MOF, **$Bi_2(2,6\text{-}Hpdc)_2(2,6\text{-}pdc)_2\cdot 2H_2O$** using 2,6-$H_2$pdc through hydrothermal process.[80] The asymmetric unit of this MOF consists of two Bi, two mono-protonated 2,6-$Hpdc^-$ ligands, two 2,6-pdc^{2-} ligands and two water units. 2,6-pdc^{2-} ligands link two Bi to form a dual-core unit, and through 2,6-$Hpdc^-$ connection into a 1D chain (Fig. 4a). The H-bonds (C5–H5A…O15) between two chains result in a 2D sheet (Fig. 4b). Moreover, 3D structure is formed by H-bonds (C18–H18A…O6) (Fig. 4c).

View Article Online
DOI: 10.1039/D0QI01052C

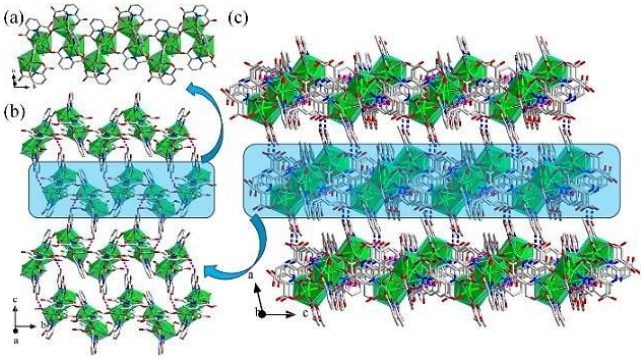

Fig. 4 (a) 1D chain of **Bi_2(2,6-Hpdc)$_2$(2,6-pdc)$_2$·2H_2O**. (b) 2D layer via H-bonds interactions. (c) The 3D supramolecular structure. Reproduced with permission from ref. 80. Copyright 2016, Elsevier.

Two MOFs, **{[Bi_2(Hbpp)(bpp)(μ-I)$_2$I$_6$](Hbpp)·CH_3OH}$_n$** (**I1**) and **[Bi(Hbpp)(Br_4)]** (**I2**) [bpp = 1,3-di(pyridin-4-yl)propane], were synthesized by Morsali group using the branch tube method.[46] In **I1**, the central bismuth atom is six-coordinated and sites in a distorted octahedron. Two iodine atoms bridge two bismuth atoms. Bismuth in **I2** is also hexacoordinated, and the central bismuth atom forms a $BiBr_4N_2$ polyhedron with a one-dimensional chain structure.

Continuously, Liu group presented three MOFs, **(Hdma)[Bi(3,5-pdc)(1,4-bdc)]·2DMF** (**J1**), **(Hdma)[Bi(2,5-TDC)$_2$]·1.5DMF** (**J2**), **[Bi(bda)$_2$$H_2O$]·xGuest** (**J3**), using four symmetric simple ligands 3, 5-H_2pdc (3,5-pyridinedicarboxylic acid), 1,4-H_2bdc, 2,5-H_2TDC (2,5-thiophenedicarboxylic acid), H_2bda by solvent-thermal method.[81] In **J1**, each 3,5-pdc^{2-} connects three Bi, forms a 2D layer through two carboxyl groups and a nitrogen, and then forms a 3D structure through 1,4-bdc^{2-}. In **J2**, there are two types of pore size 5 × 6 and 6 × 6 Å. In the 2D structure of **J3**, 11 × 11 Å channel (not including van der Waals radius) can be observed.

Using a pyridine tricarboxylate ligand, 2,4,6-pyridinetricarboxylic acid (H_3PTC), four MOFs, **[Bi(PTC)(H_2O)$_2$]** (**K1**), **(H_3O)[Bi_2(PTC)(HPTC)$_2$(H_2O)$_2$]** (**K2**), **α-[Bi(PTC)]** (**K3**), **β-[Bi(PTC)]** (**K4**) were reported by Rhauderwiek et al.[84] by a high-throughput hydrothermal process in 2018. **K1** is a layered structure. These layers are linked by H-bonds between carboxyl units and coordinated H_2O. In **K2**, the two centers Bi^{3+} constitute $BiNO_7$ and BiN_2O_6 polyhedra respectively, and the completely protonated PTC^{3-} connects them. The same layered structures like **K1**, there are four kinds of hydrogen bonds among these layers. **K3** and **K4** are all three-dimensional, and **K4** is a polycrystalline form of **K3**. In **K3**, the IBU consists of a PTC^{3-} connected $BiNO_7$ edge shared dual-core unit. **K4**, IBU is composed of $BiNO_8$ dimers with shared edges, which are connected into a one-dimensional chain and formed into a 3D structure by PTC^{3-} connection.

Adopting triazine-2,4,6-triyl-tribenzoic acid (H_3TATB), two Bi-MOFs, **Bi_2(O)(OH)(TATB)]·H_2O** (**CAU-35**) and **[Bi(TATB)]·DMF·6H_2O** (**CAU-7-TATB**) were synthesized by ligand and high-throughput method.[42] **CAU-35** was solvothermally synthesized for 5 days in a H_2O/DMF solution and **CAU-7-TATB** was prepared by microwave method for 20 minutes in a CH_3OH/DMF solution. The authors calculated and solved the structures of the two MOFs by PXRD data. In **CAU-35**, BiO_7 IBUs bridged by organic ligands to form a sheet, then these sheets are linked by intermolecular H-bonds. The structure of **CAU-7-TATB** is similar to **CAU-35**. The biggest difference is the different size of the pore contained. Through the amino functionalization of H_3TATB, 2-(4-Carboxy-3-aminophenyl)-4,6-bis(4-carboxyphenyl)-1,3,5-triazine (H_3TATB-NH_2) was obtained, and **CAU-7-TATB-NH_2** was synthesized by the same method as **CAU-7-TATB**, which is an analogue of **CAU-7**. As shown in Scheme 3, acetic anhydride, pentanhydride, succinic anhydride, phthalic anhydride and 1, 3-propane sultanone were used to modify **CAU-7-TATB-NH_2**, and a series of functional Bi-MOFs were obtained.

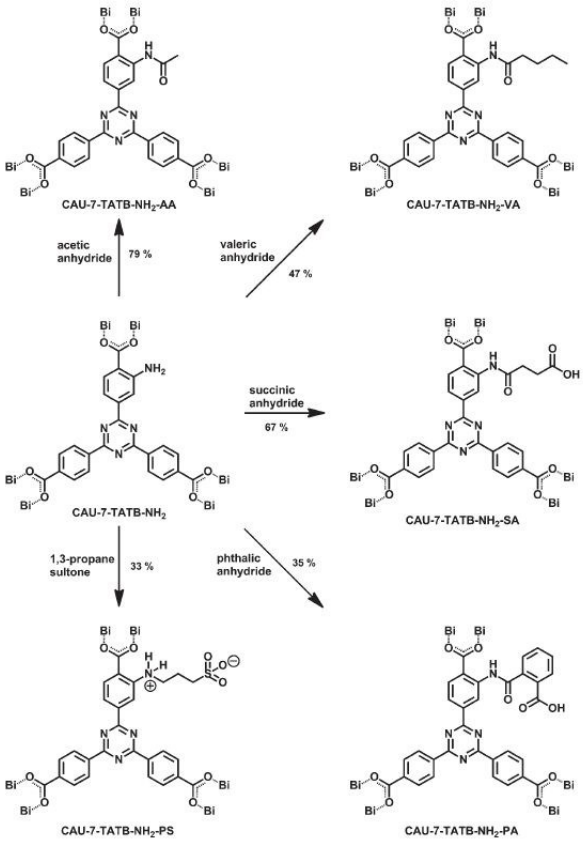

Scheme 3 Post-synthetic modification of **CAU-7-TATB-NH_2** with the respective anhydrides and 1,3-propane sultone. Degree of conversion in %. Reproduced with permission from ref. 42. Copyright 2017, American Chemical Society.

Other types of heterocyclic ligands, such as thiophenyl carboxylic acid ligands, also exhibit flexible coordination capabilities. For example, three MOFs, **Hpy[Bi(TDC)$_2$(H_2O)]·1.5H_2O** (**L1**) **(Hpy)$_3$[Bi_2(TDC)$_4$(HTDC)(H_2O)]·0.74H_2O** (**L2**),

$(Hpy)_2[Bi(TDC)_2(HTDC)]\cdot 0.36H_2O$ (**L3**), were synthesized by Adcock et al. using 2,5-thiophenedicarboxylic acid (H_2TDC), Hpy (pyridine) by normal temperature volatilized method.[85] In **L1**, center Bi^{3+} is nine coordinated with four TDC^{2-} of eight O atoms and one O atom of a water molecule. Two TDC^{2-} ligands bridged bismuth metal centers along [-1 1 0] to construct a sawtooth chain, with Bi·· Bi separation of 10.814 (4) Å. H-bonding and π-π interactions between adjacent thiophene ring stable the compound. The structure of **L2** has two central Bi ions (Bi1, Bi2). Bi1 is coordinated with ten O atoms of five ligands, and Bi2 is connected with nine O atoms of three TDC^{2-}, one $HTDC^{1-}$ ligand and one H_2O. Similar to **L1**, Bi1 and Bi2 are joined by one ligand, with Bi··Bi separation of 10.771 (11) Å. In **L3**, Bi is connected with another Bi through ligand to form a chain structure similar to **L1**, **L2**. There exist π-π interactions between $HTDC^-$ thiophene ring and pyridine ring.

Consequently, Iram et al. prepared four Bi-MOFs, **$[Bi(HMMTA)_3]_n$** (**M1**), **$[Bi(2, 6\text{-}NDA)_3]_n$** (**M2**), **$[Bi(DMP)_3]_n$** (**M3**), **$[Bi(MBA)_3]_n$** (**M4**) by conventional solution method adopting four ligands: 2-mercapto-3-methyl-4-thiazoleacetic acid (H_2MMTA), 2,6-naphthalenedicarboxylic acid (2, 6-H_2NDA), 4-mercaptobenzoic acid (H_2MBA) and 4,6-dihydroxy-2-mercaptopyrimidine (H_2DMP).[86] Nitrogen adsorption experiments (77K) showed that, they are all mesoporous materials, and the estimated BET specific surface area is **M1** > **M3** > **M4** > **M2**.

Recently, García-Sánchez group employed dithieno[3,2-b:2',3'-d]thiophene-2,6-dicarboxylic acid (H_2DTTDC) ligand to solvothermally prepare a new Bi-MOF, **$[Bi_{12}(DTTDC)_{24}]\cdot 12(Hdma)\cdot 4DMF\cdot 2H_2O$** (**IEF-5**).[87] The skeleton of **IEF-5** consists of inorganic secondary building block (SBU) $[Bi_3(\text{-}COO)_{12}]^{3-}$(Fig. 5a). Each inorganic SBU is joined by six adjacent SBU through paired parallel ligands to form a pcu type network (Fig. 5b). There are two interpenetrating networks in **IEF-5**, between which DMF and H_2O units are located (Fig. 5c). The ligand $DTTDC^{2-}$ is used as a hole transport connector for photoelectric catalytic applications.

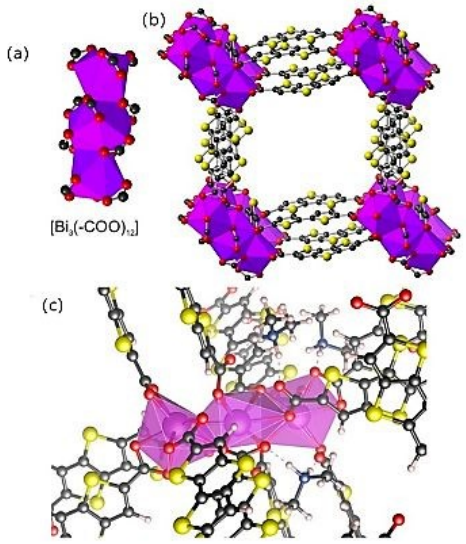

Fig. 5 (a) The structure of the SBU $[Bi_3(\text{-}COO)_{12}]^{3-}$. (b) Each SBU connecting with other six ones, forming a pcu-type network. (c) Representation of the simulated interaction of the HDMA with the framework atoms. Reproduced with permission from ref. 87. Copyright 2020, American Chemical Society.

In one word, the MOFs constructed by heterocyclic ligands are different from the phenyl ligands described in the previous part. The extra N, S and other atoms on the heterocyclic ring can greatly enhance the coordination activity. In addition to the various functional groups on the heterocyclic ligand, its own heteroatom is a good active site for metal coordination. This also leads to more complex and diverse Bi-MOFs structure.

3.3. MOFs constructed by aliphatic hydrocarbon Ligands

Although Bi-based MOFs constructed by aliphatic hydrocarbon ligands are limited, we also summarize them briefly. The chemical structures of aliphatic hydrocarbon ligands mentioned in this review are listed in Scheme 4.

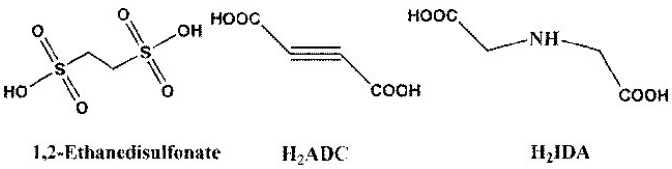

Scheme 4. The chemical structures of aliphatic hydrocarbon ligands mentioned in this review.

A 3D MOF, **$Bi(O_3SC_2H_4SO_3)_{1.5}(H_2O)_2$** was hydrothermally synthesized by Gschwind's group,[36] in which the central Bi atom is connected to the other three bismuth atoms by the organic ligands toconstruct a three-dimensional skeleton with a very minor cavity (Fig. 6).

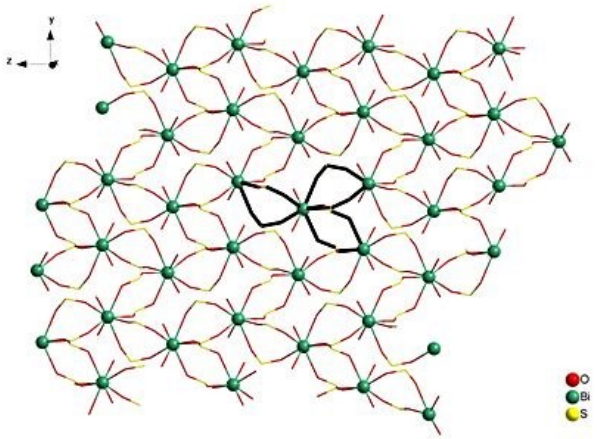

Fig. 6 The framework of **$Bi(O_3SC_2H_4SO_3)_{1.5}(H_2O)_2$**. Reproduced with permission from ref. 36. Copyright 2012, Multidisciplinary Digital Publishing Institute.

As mentioned in the previous part, **Bi-ADC-01** and **Bi-ADC-02**[38] were prepared by solution synthesis method. Each Bi(III) atom in **Bi-ADC-01** is nine-coordinated by four O atom of two chelating carboxylate units, three O atoms of three monodentate carboxylate units and two O atoms of two H_2O units, which is further joined by ADC^{2-} ligands to form a layered structure. Using the similar starting materials in preparation of **Bi-ADC-02**, only the concentration of H_2ADC is lower. A 3D structure of **Bi-ADC-02** was obtained. In this compound, a BiO_{10} polyhedron was formed, which was joined by ADC^{2-} anions to build up a 3D framework.

By employing iminodiacetic acid (H_2IDA), Gomez et al. presented a Bi-MOF, **[Bi(IDA)(IDAH)]**, which was prepared through solvothermal method.[52] In this MOF, the IDAH ligand connected the SBU along the [001] direction to form a ribbon chain. In addition, IDAH ligand connects two Bi centres to form the dimeric SBUs, and the three-dimensional supramolecular structure is constructed by strong H-bonding and π-π stacking interaction (Fig. 7).

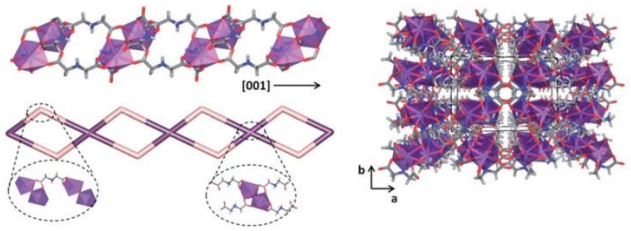

Fig. 7 Polyhedron and simplified representation of the chains (left) and crystal packing of **[Bi(IDA)(IDAH)]** (right). Reproduced with permission from ref. 52. Copyright 2018, The Royal Society of Chemistry.

3.4. MOFs constructed by ring ligands

The schematic diagram of the ring-containing ligands is shown in Scheme 5.

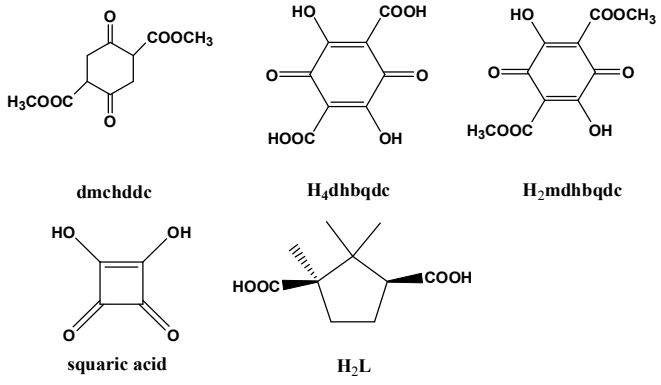

Scheme 5 The chemical structures of ring-based ligands mentioned in this review.

In 2012, three novel Bi-based MOFs, **[Bi(H_3dhbqd)(H_2dhbqd)]·2.5DMF** (**N1**) 3,6-dihydroxy-2,5-benzoquinone-1,4-dicarboxylic acid (H_4dhbqd), dimethyl 3,6-dihydroxy-2,5-benzoquinone-1,4-dicarboxylate (H_2mdhbqd) **[Bi_2(mdhbqd)(ox)$_2$(DMF)$_4$]** (**N2**) and **[Bi_2(mdhbqd)$_2$(ox)(DMF)$_4$]** (**N3**), were prepared by Zhang and coworkers by *in situ* generated anilate ligands (Scheme 6).[88] In **N1**, the central Bi (III) atom coordinates with eight O atoms of four aniline ligands. Each oxygen atom connected two Bi(III) cations to generate a diamond-like network. DMF molecules occupy the 2D channels along the a- and b-axes. The asymmetric unit of **N2** contains a bismuth, half mdhbqdc ligand, two half oxalates and two DMF. The center Bi(III) (BiO_8) displays triangular dodecahedral geometry. Similarly, in **N3**, the central bismuth atom is coordinated by eight O atoms from two mdhbqdc ligands, one ox and two DMF units. In the presence of nitric acid, the formation of **N2** is acidified into carboxylic acid, while **N3** is partially acidified. This is the first observation of the in-situ oxidation of H_4dhbqdc and H_2mdhbqdc by dmchddc. Proposed mechanism for the formation of H_2mdhbqdc, H_4dhbqdc and oxalic acid were presented by the authors.

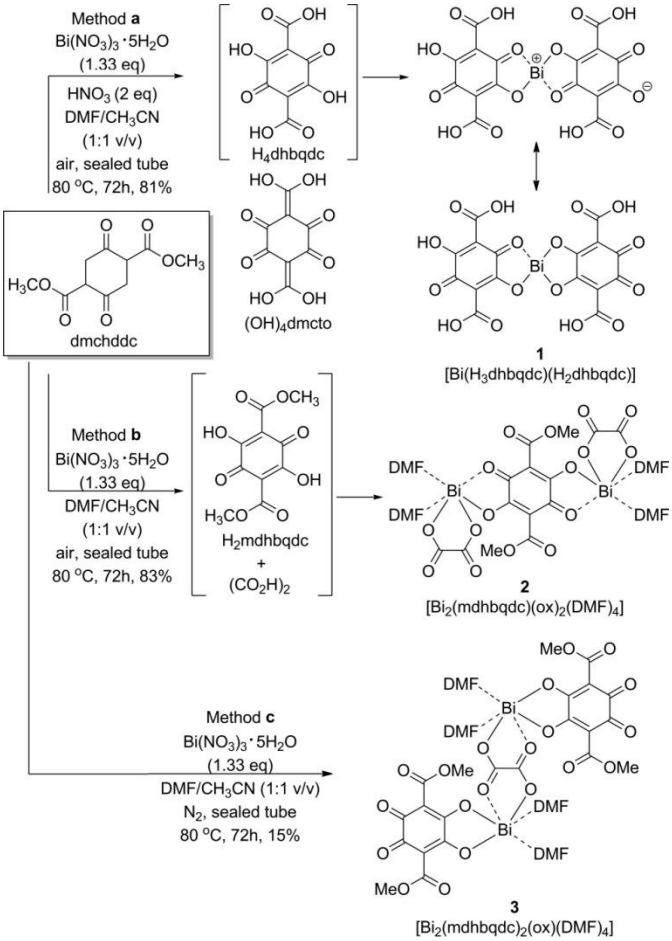

Scheme 6 Synthetic conditions for **N1-3.** Reproduced with permission from ref. 88. Copyright 2012, Royal Society of Chemistry.

In 2018, Vilela group synthesized a 2D Bi MOF by hydrothermal method using H_2L (camphor acid), **[Bi(L)(HL)]**, denotes **IEF-1**.[89] **IEF-1** has good thermal stability at 240°C. The center Bi^{3+} is coordinated with three L^{2-} and one HL^-.

Another L-based MOF, **$Bi_4Na_4L_8(EtOH)_{3.1}(H_2O)_{3.4}$** was synthesized by Wibowo et al.[77] In this MOF, the coordination spheres of the four Bi(III) ions, Bi(1)O_6, Bi(2)O_7, Bi(2)O_7, and Bi(4)O_6, are hemidirected polyhedra of nido penta-gonal bipyramid, capped nido pentagonal bipyramid, capped nido pentagonal bipyramid, and capped nido octahedron, respectively. The surroundings around the four Na^+ ions, Na(1)O_6, Na(2)O_6, Na(3)O_6 and Na(4)O_4, forming irregular octahedra, irregular monocapped square pyramids, and irregular tetrahedra. **$Bi_4Na_4L_8(EtOH)_{3.1}(H_2O)_{3.4}$** contains a zigzag chain extending along the z-direction. Nevertheless, when rotated 90° around the (-) y-axis, it is clear that this is actually a 2D structure because the bridging ligand connects the chain along the y-direction. These sheets are stacked on top of each structure in the x-axis. Na^+ ions complete the three-dimensional framework by linking these layers.

Babaryk group synthesized a MOF, **$Bi_2O_2(C_4O_4)$** by hydrothermal method using $H_2C_4O_4$ (square acid) lately, which was expressed as **IEF-3**.[90] The photochemical behavior of **IEF-3** is similar to that of α-Al_2O_3, an N-type semiconductor that absorbs ultraviolet light. Electron enrichment of **IEF-3** may be due to electron donor behavior of square anions. This fact has important implications for the modulability of molecular semiconductor properties and opens interesting new avenues for the application of photochemistry. In particular, $[Bi_2O_2]^{2+}$ semiconductors can be designed and modified by using functional substituents.

In general, both aliphatic hydrocarbon and ring ligands bear O-containing functional units, such as carboxyl, hydroxyl and ester groups, which can participate in coordination with bismuth ions, thus contributing to the formation of polytropic structures of Bi-MOFs.

4. Applications of Bi(III) MOFs

4.1. Catalytic

Bismuth-based materials are more appropriate candidates for catalysis. Nevertheless, a little attention has been paid to Bi-based MOFs in terms of catalysts. Nguyen et al. used **Bi-bdc** for photocatalytic degradation of RhB.[50] The experimental results illustrated that the photocatalytic activity of **Bi-bdc-MW** was higher than that of **Bi-bdc-ST**, and the degradation of RhB reached 99.44% after 360 min of lighting. The high photocatalytic activity may be due to its layered structure, high specific surface area and oxygen deficiency, as well as good electron hole separation. Also, Ye and coworkers utilized **$\{[Bi(BTC)(H_2O)_2]\cdot H_2O\}_n$** for photocatalytic degradation of methyl orange (MO), and the photocatalysis effect was the best under acidic (pH=3) conditions with a content of 0.60 $g\cdot L^{-1}$ (reaching equilibrium in about one hour).[56] Huang group found that **$Bi_2(2,6\text{-}Hpdc)_2(2,6\text{-}pdc)_2\cdot 2H_2O$** is a good material to degrade RhB (97%, UV irradiation 120min) and MB (91%, UV irradiation 120 min) under UV irradiation.[80] Such results proved that Bi-MOFs have the potential for efficient photocatalytic degradation of organic dyes.

Besides, Wang and coworkers reported that **$[Bi(BTC)(DMF)]\cdot DMF\cdot 2CH_3OH$** could photocatalyze water to produce oxygen,[53] and produce oxygen (about 880 $\mu L\cdot h^{-1}$) under ultraviolet and visible light irradiation.

Xiao et al. conducted an in-depth study on the photocatalytic hydrogen production performance of **Bi-TBAPy**, and the results demonstrated that **Bi-TBAPy** had good stability and hydrogen production capacity.[70] The optimal hydrogen evolution rate of this MOF with load of 2.0 wt% Pt was 140 $\mu mol\cdot h^{-1}\cdot g^{-1}$. As denoted in Fig. 8, first, under light conditions, the MOF absorbs light to produce electron and hole. Consequently, excited electrons are consumed across two pathways. In one pathway, electrons are transferred to nearby Bi^{3+} ions through the LMCT mechanism, and after that transferred to the cocatalyst. In another approach, the excited electrons are directly transferred to the Pt particles. Then, the deposited Pt serves as an active site for the catalytic hydrogen production of H_2O, and the light-generated holes are concurrently consumed by the sacrificial reagent TEOA (triethanolamine). Their research provides new ideas and directions for the application design and operation of Bi-MOFs in photocatalysis.

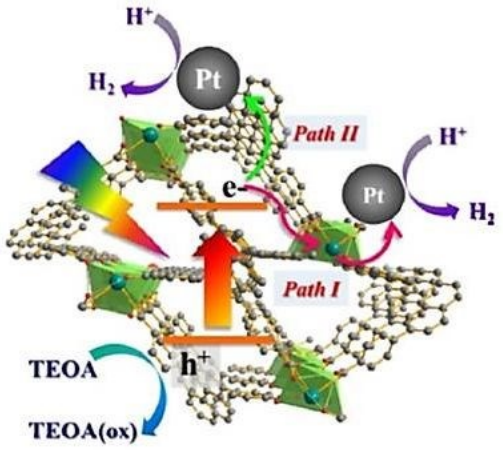

Fig. 8 Proposed mechanism of photocatalytic H_2 evolution over Bi-TBAPy. Reproduced with permission from ref. 70. Copyright 2019, Elsevier.

In 2020, Zhang group adopted solvothermal synthesis to obtain a MOF, **Bi(BTC)(DMF)**, and explored its electrochemical reduction of CO_2.[59] The average Faraday efficiency of formic acid was 93.0% after continuous electrolysis for 12 hours. In the same year, Lamagni et al. used another Bi-MOFs **CAU-7** for photocatalytic reduction of CO_2.[72] They discovered that Faradaic efficiency was as high as 95(3)% when **CAU-7** derived materials selectively reduced CO_2 at 770 mV overvoltage. In addition, in mass activity, it is superior to most Bi-based catalysts reported recently and can reach 158(11) $A\cdot g^{-1}$ under 770 mV overvoltage (comparable to the best Sn-based electrocatalyst). The **CAU-7** derivative material catalyzed the

reduction of CO_2 to formate, and its own structure changed to form bismuth-based nanoparticles. Although the structure of **CAU-7** has changed, as a former catalyst, **CAU-7** forms a metal active center evenly distributed in the organic network structure, which opens a new way for the development of various kinds of high quality active metal-based materials.

Moreover, Köppen and coworkers selected **CAU-17** as the heterogeneous catalyst to catalyze the ring-opening of ethylene oxide.[54] The results revealed that it could convert phenyl ethylene oxide to 2-methoxy-2-phenylethanol with high selectivity. And, through the study of acetal reaction and esterification reaction, Sushrutha et al. noted that **[pip][Bi(2,6-Hpdc)(2,6-pdc)]·H_2O** has higher catalytic activity for similar organic reaction.[79]

In general, MOFs based on bismuth have catalytic activity and can be used as promising candidates for high-efficiency catalysts.

4.2. Fluorescence

In addition to be used as a catalyst, Bi-MOFs have also been extensively studied for its own fluorescence properties. Feyand and coworkers carried out fluorescence properties and doping experiments on **Bi_2(O)(Pyr)(H_2O) (C1)**, **Bi(HPyr) (C2)**, **Bi(HPyr)** (**C3**).[51] At the excitation wavelength of 254/366 nm, **C1** and **C2** exhibit doughty blue luminescence and **C3** has pale green luminescence. Similar structures can be seen in **C2** and **C3**, but with different fluorescence characteristics. However, the structures of **C1** and **C2** are different, but the fluorescence properties are the same.

In 2018, Xu et al. prepared Eu^{3+} or Tb^{3+} single-doped and co-doped compounds based on **CAU-17**, and conducted detailed luminescence performance studies (Fig. 9).[57] It was found that Eu^{3+} or Tb^{3+} mono-doped Bi complexes have high sensing properties for Fe^{3+} and $Cr_2O_7^{2-}$ ions, and have significant solvent-dependent luminescence response to certain organic pollutants. This further proves that Ln-functionalized MOFs are promising candidates for designing new luminescent materials and sensors.

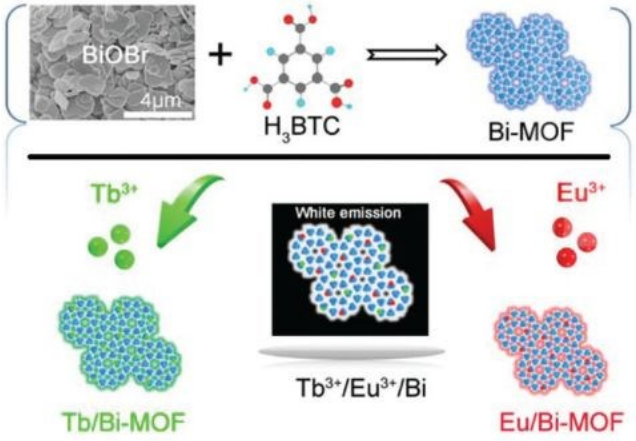

Fig. 9 Schematic diagram of the synthesis of Eu/Tb ion functionalized Bi-MOF from the BiOBr precursor for luminescence applications. Reproduced with permission from ref. 57. Copyright 2018, Royal Society of Chemistry.

[(Hdma)Bi(1,4-ndc)$_2$(DMF)]$_n$·nDMF (**E1**) was doped with Eu^{3+} (**E2**), Tb^{3+} (**E3**), Sm^{3+} (**E4**), Dy^{3+} (**E5**), and investigated by photoluminescence (PL) and cathode ray luminescence (CL).[65] The results displayed that doping rare earth can effectively improve the CL performance of the complex, among which Eu^{3+} doped **E2** is expected to be an excellent CL scintillation material in FED electronic devices of field emission display.

Photoluminescence, biological imaging and fluorescence sensing were performed on the **Bi(TBAPy)** by Guan group.[71] Studies illustrated that **Bi(TBAPy)** had low toxicity and a unique fluorescence behavior towards biothiol units (Cysteine; Glutathione; Homocysteine), which could specifically detect biothiol molecules.

Wibowo et al. examined the fluorescence performance of **Bi(2,5-pdc)(2,5-Hpdc)(H_2O)** (**F1**).[75] The emission spectrum of **F1** (λex = 369 nm, emits green light with a maximum peak at 533 nm and a broad shoulder at 570 nm) is red-shifted in comparison to that of the as-received 2,5-H_2pdc ligand (λex = 390 nm, emits pale-green light with a maximum emission around 518 nm). Also, fluorescence studies on **Bi(2,5-pdc)$_2$(H_3O^+)(H_2O)$_{0.83}$** have shown when excited at 340 nm, it emitted pale blue light with maximum peak at 481 nm and a broad shoulder at 513 nm.[76] It is likely due to LMCT and/or $^1P_1 \rightarrow {}^1S_0$ and $^3P_1 \rightarrow {}^1S_0$ transitions of s^2 electrons of Bi^{3+}.

Thirumurugan group has conducted the fluorescence performance of **Bi(2,6-pdc)(2,6-pdcme)(CH_3OH)** (**G4**), **[LiBi(2,6-pdc)$_3$(H_2O)]·2(Hdma)** (**G5**) and Tb^{3+}, Eu^{3+} co-doped compounds.[78] The emission spectra of the undoped compounds **G4** and **G5** showed a broad peak centered at ~427/456 nm due to intra-ligand luminescence (n ← π*)/(π ← π*) or charge transfer transitions. **G4a** (5 mol% Tb and 5 mol% Eu) and **G5a** (5 mol% Tb and 5 mol% Eu) revealed excitation spectra with a maximum band at 279 and 370 nm for **G4a** and at 292 and 335 nm for **G5a**.

The luminescence properties of **(Hdma)[Bi(3,5-pdc)(bdc)]·2DMF (J1)** and its rare earth doped (Tb^{3+}, Eu^{3+}, Dy^{3+} doped during synthesis) compounds were explored by Liu group.[81] **J1** emitted blue light (λex = 313 nm). Tb^{3+}, Eu^{3+} and Dy^{3+} doped **J1** emitted strong green, red and blue light at 330 nm, respectively. The detection of nitro explosives (TNP= 2,4,6-trinitrophenyl; 2,4-DNP = 2,4-dinitrophenol; 4-NP = 4-nitrophenol) with **J1** as fluorescent probe was further studied. When **J1** is excited at 313 nm, it shows strong emission at 414 nm. However, fluorescence quenching can be observed by adding TNP, 2,4-DNP and 4-NP, and then **J1** can be used as a fluorescent probe to detect nitro explosives.

Rhauderwiek et al. performed fluorescence studies on four MOFs, **[Bi(PTC)(H_2O)$_2$]** (**K1**), **(H_3O)[Bi_2(PTC)(HPTC)$_2$(H_2O)$_2$]** (**K2**), **α-[Bi(PTC)]** (**K3**), **β-[Bi(PTC)]** (**K4**).[84] **K3** and **K4** have no fluorescence properties. **K1** emits yellow light under UV light, with a maximum emission wavelength of 570 nm (excitation

wavelength of 343 nm), while **K2** emission band is located at 483 nm (excitation wavelength of 347 nm). Within the range of blue-green spectrum, **K1** and **K2** show spectral differences, which may be related to the different coordination environments.

Adcock and coworkers have investigated the fluorescence properties of the lanthanide-ions doped compounds of **Hpy[Bi(TDC)$_2$(H$_2$O)]·1.5H$_2$O** (**L1**) and **(Hpy)$_2$[Bi(TDC)$_2$(HTDC)]·0.36H$_2$O** (**L3**).[85] The specific operation method is as follows: **Hpy[Bi$_{1-x}$Ln$_x$(TDC)$_2$(H$_2$O)]·1.5H$_2$O** (**Bi$_{1-x}$Ln$_x$-L1**) (Ln = Nd, Sm, Eu, Tb, Dy, Yb) and **[Bi$_{0.99}$Eu$_{0.01}$(TDC)$_2$(HTDC)(Hpy)$_2$]**(**Bi$_{0.99}$Eu$_{0.01}$-L3**) were prepared by adding rare earth nitrate solution in the process of **L1**, **L3** synthesis. The rare earth doping proportion of **L1**, **L3** was determined by ICP-MS. After lanthanide doping, they showed different fluorescent properties, which provided a new perspective on the development of Bi-MOFs design strategies that can be doped with rare earths as photoluminescent materials or fluorescent probes.

Four complexes, **[Bi(HMMTA)$_3$]$_n$** (**M1**), **[Bi(2, 6-NDA)$_3$]$_n$** (**M2**), **[Bi(DMP)$_3$]$_n$** (**M3**), **[Bi(MBA)$_3$]$_n$** (**M4**) all emitted blue light.[86]

In a word, these Bi-MOFs showed varied fluorescence characteristics and fluorescence recognition ability, which is worth further study.

4.3. Biology and medicine

Due to the low toxicity of such MOFs, there is great concern about their application in biology and medicine. For instance, Burrows et al. conducted drug release for deferiprone and against H. pylori (strain SS1) studies on **[Bi$_2$(1,4-bdc)(dfp)$_4$(H$_2$O)$_2$]·2DMF** (**B2**), **[Bi$_2${1,4-bdc-(OH)$_2$}(dfp)$_4$(H$_2$O)$_2$]·2DMF** (**B4**).[49] The results demonstrated that **B2**, **B4** released deferiprone quickly under acid or phosphate buffered saline (PBS) treatment. And, **B2**, **B4** also showed excellent antibacterial activity, inhibiting the reproduction of H. pylori. In this potential double-acting mode, both the ligand and the metal center play different biological roles, which have broad implications for other systems.

Gomez group found that **Bi(Pyr)$_{0.5}$(2,2'-bipy)(NO$_3$)(DMF)]** with a strong antibacterial effect on Escherichia coli, Salmonella typhimurium and Pseudomonas aeruginosa.[52]

Fairen-Jimenez's and coworkers first used Bi-MOF **CAU-7** as DDSs (Drug Delivery Systems) for the delivery of the anticancer drugs sodium DCA (dichloroacetate) and α-CHC (α-cyano-4-hydroxycinnamic acid).[73] The results denoted that DCA can reach 33% load on CAU-7 and 9% load on α-CHC. DCA and α-CHC were released at 17 and 31 days, respectively, and showed better anticancer efficacy than free drugs.

Iram et al. performed antibacterial research on **M1**, **M2**, **M3** and **M4**,[86] and the results displayed that **M1**, **M3** and **M4** showed higher antibacterial activity to bacillus cereus.

Although Bi-MOF shows excellent antibacterial properties and can be used in medicine, biology, etc, the related researches are very limited. In the future, people need to design and prepare more Bi-MOFs to study their applications in this field.

4.4. Adsorption

Ouyang and coworkers first reported the use of **CAU-17** to selectively adsorb SeO_3^{2-} from aqueous solution.[55] It exhibits excellent SeO_3^{2-} selectivity, ultra-high adsorption capacity of 255.3 mg/g, and relatively mild working conditions (pH 4-11).

Sun et al. uncovered that **[Bi(BTC)(H$_2$O)]·H$_2$O** had excellent detection ability for iron(III) ion (detection limit: 1.59 μM) and $Cr_2O_7^{2-}$ (detection limit: 1.64 μM).[58] Savage group researched the gas adsorption properties of **[Bi2(BPTC)1.5]** (**NOTT-220a**).[60] The results illustrated that it had a good adsorption of gravimetric gas, 14.1 and 8.2 wt % at 195 and 293 K for CH_4 at 20 bar, 40.7 and 37.9 wt % at 273 and 293 K for CO_2.

Köppen and his colleagues carried out adsorption experiments on three MOFs, **CAU-31**- **CAU-33**.[64] **CAU-31** and **-32** did not show N_2 absorption, and the Isotherm of Type I of **CAU-33** (77 K) was observed. They also conducted exploratory experiments on their stability, and the three complexes had good thermal and chemical stability.

Thirumurugan et al. did the adsorption experiments on N_2, H_2 and CO_2 of **[Bi(2,6-pdc)$_3$]·3(Hdma)·2H$_2$O** (**G2**), **Bi(2,6-pdc)(2,6-pdcme)(CH$_3$OH)** (**G4**), **[LiBi(2,6-pdc)$_3$(H$_2$O)]·2(Hdma)** (**G5**) and **Li$_5$Bi(2,6-pdc)$_4$(H$_2$O)$_2$** (**G6**).[78] They all have a good adsorption of CO_2. **G6** reveals the best adsorption performance with a maximum value of 140 cc g^{-1} (~6 mmol g^{-1}) of CO_2. The H_2 sorption isotherms indicate a significantly higher uptake (3.1 wt% at 760 Torr) for **G5**. The approximate CO_2/N_2 selectivities on volumetric uptake at 275 K and 600 Torr are 2, 1.7, 60 and 23 for **G2**, **G4**, **G5** and **G6** respectively.

In 2018, the lead ion adsorption of **CAU-7-TATB** was investigated by Zhang et al.,[82] which had highly selective for lead ions. So **CAU-7-TATB** can be used as a new type of lead ion adsorbent. Lately, Zhang et al. used this MOF to selectively oxidize alcohols.[83]

In summary, we briefly summarized the syntheses, structures and application of Bi-based MOFs that have been reported in recent years. We found that Bi-based MOFs have the following unique advantages. First of all, Bi-MOFs exhibit good chemical stability, which provides a prerequisite for their wide application. Secondly, because bismuth has a large radius, and high affinity for oxygen and nitrogen atoms, the central Bi(III) atom always has high coordination number, which is conducive to the formation of complicated structural MOFs. Thirdly, Bi-MOFs indicated various applications, such as being used as the catalytic materials for high-efficiency photocatalysis, as a carrier for drug transport, for the treatment of certain diseases; doping with lanthanides for optical applications etc. Nevertheless, the research of Bi-MOFs is still in its infancy, and it needs more in-depth research by researchers.

5. Conclusions

Due to the low toxicity and environmental friendliness of Bi atom, more and more Bi-based MOFs have been reported. However, the relevant research is still very limited, research scope needs to be further deepened and expanded. The following points need to be paid special attention: First, from the perspective of the existing Bi(III) MOFs, the functionalization of organic ligands has a great impact on the subsequent structures. More attention should be paid to organic ligands with sulfonic acid and phosphate groups carrying multiple oxygen atoms and organic ligands with multiple nitrogen atoms such as imidazole, triazole, tetrazazole, etc. Secondly, because coordination of bismuth ion is easy to be affected by external conditions, the emerging microwave, mechanochemistry and sonochemistry methods should be more adopted to prepare more complicated MOFs. Third, based on the abound structures and high stability of Bi-MOFs, their application should be expanded, such as in the field of energy acting as proton conductors and so on. Finally, the application of such MOFs in drug delivery, especially in cancer treatment, heavy metal removal and chemical sensors, needs to be deepened. Therefore, we have reasons to believe that in future research, Bi-based MOFs will surely come out on top.

Conflicts of interest

There are no conflicts to declare.

Acknowledgements

The authors acknowledge the National Natural Science Foundation of China (22071223).

References

1 L. Chen, H.-F. Wang, C. Li, Q. Xu, Bimetallic metal-organic frameworks and their derivatives, *Chem. Sci.*, 2020, 5369-5403.

2 X. Lian, Y. Fang, E. Joseph, Q. Wang, J. Li, S. Banerjee, C. Lollar, X. Wang, H.-C. Zhou, Enzyme-MOF (metal-organic framework) composites, *Chem. Soc. Rev.*, 2017, **46**, 3386-3401.

3 M. Wen, K. Mori, Y. Kuwahara, T. An, H. Yamashita, Design and architecture of metal organic frameworks for visible light enhanced hydrogen production, *Appl. Catal. B*, 2017, **218**, 555-569.

4 Q. Yang, Q. Xu, H.-L. Jiang, Metal-organic frameworks meet metal nanoparticles: synergistic effect for enhanced catalysis, *Chem. Soc. Rev.*, 2017, **46**, 4774-4808.

5 H. Daglar, S. Keskin, Recent advances, opportunities, and challenges in high-throughput computational screening of MOFs for gas separations, *Coord. Chem. Rev.*, 2020, **422**, 213470.

6 D. Yang, B. C. Gates, Catalysis by metal organic frameworks: perspective and suggestions for future research, *ACS. Catal.*, 2019, **9**, 1779–1798.

7 C. Zhao, X. Dai, T. Yao, W. Chen, X. Wang, J. Wang, J. Yang, S. Wei, Y. Wu, Y. Li, Ionic exchange of metal–organic frameworks to access single nickel sites for efficient electroreduction of CO_2, *J. Am. Chem. Soc.*, 2017, **139**, 8078–8081.

8 G.P. Li, G. Liu, Y.Z. Li, L. Hou, Y.Y. Wang, Z.H. Zhu, Uncommon pyrazoyl-carboxyl bifunctional ligand-based microporous lanthanide systems: sorption and luminescent sensing properties, *Inorg. Chem.*, 2016, **55**, 3952-3959.

9 B. Li, J. Zhou, F.Y. Bai, Y.H. Xing, Lanthanide-organic framework based on a 4,4-(9,9-dimethyl-9H-fluorene-2,7-diyl) dibenzoic acid: synthesis, structure and fluorescent sensing for a variety of cations and anions simultaneously, *Dyes Pigments*, 2020, **172**, 107862.

10 Y.-J. Li, T.-Y. Gai, Y.-J. Lin, W.-J. Zhang, K. Li, Y. Liu, Y.-Q.Duan, B.-J. Li, J. Ding, J.-P. Li, Eight Cd(II) coordination polymers with persistent room-temperature phosphorescence: intriguing dual emission and time-resolved afterglow modulation, *Inorg. Chem. Front*., 2019, **7**, 777-785.

11 Y.-P. Hao, C.-P. Yue, B.-N. Jin, Y.-L. Lv, Q.-K. Zhang, J.-P Li, Z.-Y. Liu, H.-W. Hou, Syntheses, structures, luminescent properties and antibacterial activities of seven polymers based on an asymmetric triazole dicarboxylate ligand, *Polyhedron*, 2018, 139, 296-307.

12 J.-P. Li, X.-T. Wang, R.-Y. Li, W.-J. Zhang, H.-N. Bai, Y. Liu, Z.-C. Liu,T.-T. Yu, Z.-Y. Liu, Y.-P Yang, Y. Zhu, Twelve cadmium(ii) coordination frameworks with asymmetric pyridinyl triazole carboxylate: syntheses, structures, and fluorescence properties, *Cryst. Growth Des*, 2019, **19**, 3785-3806.

13 K. Adil, Y. Belmabkhout, R.S. Pillai, A. Cadiau, P.M. Bhatt, A.H. Assen, G. Maurin, M. Eddaoudi, Gas/vapour separation using ultra-microporous metal–organic frameworks: insights into the structure/separation relationship, *Chem. Soc. Rev.*, 2017, **46**, 3402–3430.

14 S. Yang, A. J. Ramirez-Cuesta, R. Newby, V. Garcia-Sakai, P. Manuel, S. K. Callear, S. I. Campbell, C. C. Tang, M. Schröder, Supramolecular binding and separation of hydrocarbons within a functionalized porous metal–organic framework, *Nature Chem.*, 2015, **7**, 121–129.

15 J.-J. Cheng, S.-M. Wang, Z. Shi, H. Sun, B.-J. Li, M.-M. Wang, M.-Y. Li, J.-P. Li, Z.-Y. Liu, Five metal-organic frameworks based on 5-(pyridine-3-yl)pyrazole-3-carboxylic acid ligand: Syntheses, structures and properties, *Inorg. Chim. Acta*, 2016, **453**, 86-94.

16 X.-X. Xie, Y.-C. Yang, B.-H. Dou, Z.-F. Li, G. Li. Proton conductive carboxylate-based metal-organic frameworks. *Coord. Chem. Rev*., 2020, **403**, 213100.

17 X. -L. Sun, W. -H. Deng, H. Chen, H. -L. Han, J. M. Taylor, C. -Q. Wan, G. Xu, A metal–organic framework impregnated with a

binary ionic liquid for safe proton conduction above 100°C. *Chem. Eur. J*., 2017, **23**, 1248-1252.

18 Y. Qin, X.-Y. Wang, W.-P. Xie, Z.-F. Li, G. Li, Structural effect on proton conduction in two highly stable disubstituted ferrocenyl carboxylate frameworks, *Inorg. Chem*., 2020, **59**, 10243–10252.

19 X. Chen, G. Li, Proton conductive Zr-MOFs, *Inorg. Chem. Front.,* 2020, **7**, 3765-3784.

20 Z.-C. Guo, Z.-Q. Shi, X.-Y. Wang, Z.-F. Li, G. Li, Proton conductive covalent organic frameworks, *Coordin. Chem. Rev*., 2020, **422**, 213465.

21 M.-S. Yao, X.-J. Lv, Z.-H. Fu, W.-H. Li, W.-H. Deng, G.-D. Wu, G. Xu, Layer-by-layer assembled conductive metal–organic frameworknanofilms for room-temperature chemiresistive sensing*, Angew. Chem. Int. Ed*., 2017, **56**, 16510 –16514.

22 R.-L. Liu, W.-T. Qu, B.-H. Dou, Z.-F. Li, G. Li, Two proton conductive 3D Ln(III) MOFs for formic acid impedance sensing. *Chem-Asian J.*, 2020, **15**, 182 – 190.

23 R.-L. Liu, Y.-R. Liu, S.-H. Yu, C.-L. Yang, Z.-F. Li, G. Li, A highly proton conductive 3D ionic cadmium-organic framework for ammonia and amines impedance sensing, *ACS Appl. Mater. Interfaces*, 2019, **11**, 1713−1722

24 Z.-B. Sun, S.-H. Yu, L.-L. Zhao, J.-F. Wang, Z.-F. Li, G. Li, A highly stable two-dimensional copper(II)-organic framework for proton conduction and ammonia impedance sensing, *Chemistry - Eur. J*., 2018, **24**, 10829– 10839.

25 R.-M. Wang, H.-Y. Li, T. K. Ip, H.-Z. Sun, Bismuth drugs as antimicrobial agents, *Adv. Inorg. Chem.*, 2019, **75**,183-205

26 H. Alkim, A. R. Koksal, S. Boga, I. Sen, C. Alkim, Role of bismuth in the eradication of helicobacter pylori, *Am. J. Ther.*, 2016, **0**, 1–7.

27 P. Malfertheiner, F. Megraud, C. O'Morain, F. Bazzoli, E. El-Omar, D. Graham, R. Hunt, T. Rokkas, N. Vakil, E. J. Kuipers, Current concepts in the management of helicobacter pylori infection: the maastricht III consensus report free, *E. J. Gut.*, 2007, **56**, 772-781.

28 W. D. Chey, G. I. Leontiadis, C. W. Howden, S. F. Moss, Acg clinical guideline: treatment of helicobacter pylori Infection. *Am. J. Gastroenterol.*, 2017, **112**, 212-239.

29 G. G. Briand, N. Burford, Bismuth compounds and preparations with biological or medicinal relevance, *Chem. Rev.*, 1999, **99**, 2601−2657.

30 R. Kannan, S. Kumar, A. P. Andrews, E. D. Jemmis, A. Venugopal, Consequence of Ligand bite angle on bismuth lewis acidity, *Inorg. Chem.*, 2017, **56**, 9391–9395.

31 J. Sanderson, C. A. Bayse, The lewis acidity of bismuth (III) halides: a DFT analysis, *Tetrahedron*, 2008, **64**,7685-7689

32 Y. Yang, R.-Z. Ouyang, L.-N. Xu, N. Guo, W.-W. Li, K. Feng, L. Ouyang, Z.-Y. Yang, S. Zhou, Y.-Q. Miao, Review: bismuth complexes: synthesis and applications in biomedicine, *J. Coord. Chem.*, 2015, **68**, 379-397.

33 X.-Y. Zhao,X. Chen, J.-C. Hu, Composition-dependent dual halide anion-doped bismuth terephthalate hybrids for enhanced pollutants removal author links open overlay panel, *Microporous Mesoporous Mat.*, 2017, **244**, 284-290.

34 S.-M. Zhou, D.-K. Ma, P. Cai, W. Chen, S. -M. Huang, $TiO_2/Bi_2(BDC)_3/BiOCl$ nanoparticles decorated ultrathin nanosheets with excellent photocatalytic reaction activity and selectivity, *Mater. Res. Bull.*, 2014, **60**, 64-71.

35 D. T. Trana, D. Chua, A. G. Oliverb, S. R. J. Oliverb, A 3-D bismuth–organic framework containing 1-D cationic inorganic $[Bi_2O_2]^{2+}$chains, Inorg. *Chem. Commun.*, 2009, **12**, 1081-1084.

36 F. Gschwind, M. Jansen, An unusual bismuth ethanedisulfonate network, *Crystals*, 2012, **2**, 1374-1381.

37 G.-Z. Wang, Q.-L. Sun, Y.-Y. Liu, B.-B. Huang, Y. Dai, X.-Y. Zhang, X.-Y. Qin, A bismuth-based metal–organic framework as an efficient visible-light-driven photocatalyst, *Chem. Eur. J.*, 2014, **20**, 1–5.

38 S. Busch, I. Stein, U. Ruschewitz, Hydrate isomerism in coordination polymers of bismuth and acetylenedicarboxylate, Z. Anorg. *Allg. Chem.*, 2012, **638**, 1–5.

39 M. S. Roodsari, B. Shaabani, B. Mirtamizdoust, M. Dusek, K. Fejfarova, Sonochemical synthesis of bismuth (III) nano coordination compound and direct synthesis of Bi_2O_3 nanoparticles from a Bismuth (III) Nano Coordination Compound precursor, *J. Inorg. Organomet. Polym. Mater.*, 2015, **25,** 1226–1232.

40 A. K. Inge, M. Köppen, J. Su, M. Feyand, H.-Y. Xu, X.-D. Zou, M. O'Keeffe, N. Stock, Unprecedented topological complexity in a metal−organic framework constructed from simple building units, *J. Am. Chem. Soc.*, 2016, **138**, 1970−1976.

41 M. Feyand, E. Mugnaioli, F. Vermoortele, B. Bueken, J. M. Dieterich, T. Reimer, U. Kolb, D. D. Vos, N. Stock, Automated diffraction tomography for the structure elucidation of twinned, sub-micrometer crystals of a highly porous, catalytically active bismuth–metal–organic framework, *Angew. Chem. Int. Ed.*, 2012, **51**, 1 – 5.

42 M. Köppen, O. Beyer, S. Wuttke, U. Lüning, N. Stock, Synthesis, functionalisation and post-synthetic modification of bismuth metal–organic framework s, *Dalton Trans.*, 2017, **46**, 8658.

43 L. Tröbs, M. Wilke, W. Szczerba, U. Reinholz, F. Emmerling, Mechanochemical synthesis and characterization of two new bismuth metal organic frameworks, *CrystEngComm.*, 2014, **16**, 5560–5565.

44 S. Iram, M. Imran, F. Kanwal, S. Latif, Z. Iqbal, Bismuth and lead based metal organic frameworks: morphological, luminescence and brunauer-emmett-teller (BET) studies, *Materials Science-Poland*, 2020, **38**, 132-137.

45 M. Sanchez-Salaa, O. Vallcorbab, C. Domingoc, J. A. Ayllóna, Acetic acid as a solvent for the synthesis of metal–organic frameworks based on trimesic acid, *Polyhedron*, 2019, **170**, 458–462.

46 X.-W. Yan, E. Haji-Hasanib, A. Morsalic, Syntheses and structural characterization of two new nanostructured Bi (III)

supramolecular polymers via sonochemical method, *Ultrason. Sonochem.*, 2016, **31**, 129–134.

47 Y. Hanifehpour, B. Mirtamizdoust, M. Hatami, B. Khomami, S. W. Joo, Synthesis and structural characterization of new bismuth (III) nano coordination polymer: a precursor to produce pure phase nano-sized bismuth (III) oxide, *J. Mol. Struct.*, 2015, **1091**, 43-48.

48 A. Thirumurugan, A. K. Cheetham, Anionic Metal–organic frameworks of bismuth benzenedicarboxylates: synthesis, structure and ligand-sensitized photoluminescence, *Eur. J. Inorg. Chem.*, 2010, **24**, 3823–3828.

49 A. D. Burrows, M. Jurcic, M. F. Mahon, S. Pierrat, G. W. Roffe, H. J. Windle, J. Spencer, Bismuth coordination networks containing deferiprone: synthesis, characterisation, stability and antibacterial activity. *Dalton Trans.*, 2015, **44**, 13814-13817.

50 V. H. Nguyen, T. D. Nguyen, T. V. Nguyen, Microwave-assisted solvothermal synthesis and photocatalytic activity of bismuth(III) based metal–organic framework, *Top. Catal.*, 2020.

51 M. Feyand, M. Kçppen, G. Friedrichs, N. Stock, Bismuth tri- and tetraarylcarboxylates: crystal structures, In situ X-ray Diffraction, intermediates and luminescence, *Chem. Eur. J.*, 2013, **19**, 12537 – 12546.

52 G. E. Gomez, R. F. D'vries, D. F. Lionello, L. M. Aguirre-Díaz, M. Spinosa, C. S. Costa, M. C. Fuertes, R. A. Pizarro, A. M. Kaczmarek, J. Ellena, L. Rozes, M. Iglesias, R. Van Deun, C. Sanchez, M. A. Monge, G. J. A. A. Soler-Illia, Exploring physical and chemical properties in new multifunctional indium-, bismuth-, and zinc-based 1D and 2D coordination polymers, *Dalton Trans.*, 2018, **47**, 1808–1818.

53 G.-Z. Wang, Y.-Y. Liu, B.-B. Huang, X.-Y. Qin, X.-Y. Zhang, Y.Dai, A novel metal–organic framework based on bismuth and trimesic acid: synthesis, structure and properties, *Dalton Trans.*, 2015, **44**, 16238–16241.

54 M. Köppen, A. Dhakshinamoorthy, A. K. Inge, O. Cheung, J. Ångström, P. Mayer, N. Stock, Synthesis, transformation, catalysis and gas sorption investigations on the bismuth metal-organic framework CAU-17, *Eur. J. Inorg. Chem.*, 2018, **30**, 3496-3503.

55 H. Ouyang, N. Chen, G.-J. Chang, X.-L. Zhao, Y.-Y. Sun, S. Chen, H.-W. Zhang, D.-J. Yang, Selective capture of toxic SeO_3^{2-} by bismuth-based metal-organic frameworks, *Angew. Chem. Int. Ed.*, 2018, **57**, 13197-13201.

56 F. Ye, Z.-X. Wei, J.-F. Song, X.-H. Wu, P. Yue, Synthesis, characterization, and photocatalytic properties of bismuth(III)-benzene-1,3,5-tricarboxylate, *Z. Anorg. Allg. Chem.*, 2017, **643**, 669–674.

57 L.-F. Xu, Y. Xu, X.-L. Li, Z.-P. Wang, T. Sun, X. Zhang, Eu^{3+}/Tb^{3+} functionalized Bi-based metal–organic frameworks toward tunable white-light emission and fluorescence sensing applications, *Dalton Trans.*, 2018, **47**, 16696–16703.

58 Y. Sun, N. Zhang, Q.-L. Guan, C.-H. Liu, B. Li, K.-Y. Zhang, G.-H. Li, Y.-H. Xing, F.-Y. Bai, L.-X. Sun, Sensing of $Fe^{3+}$and $Cr_2O_7^{2-}$in water and white light: synthesis, characterization, and fluorescence properties of a crystalline bismuth-1,3,5-benzenetricarboxylic acid framework, *Cryst. Growth Des.*, 2019, **19**, 7217−7229.

59 X.-R. Zhang, Y.-X. Zhang, Q.-Q. Li, X.-D. Zhou, Q.-Y. Li, J. Yi, Y.-Y. Liu, J.-J. Zhang, Highly efficient and durable aqueous electrocatalytic reduction of CO_2 to HCOOH with a novel bismuth–MOF: experimental and DFT studies, *J. Mater. Chem. A*, 2020, **8**, 9776–9787.

60 M. Savage, S.-H. Yang, M. Suyetin, E. Bichoutskaia, W. Lewis, A. J. Blake, S. A. Barnett, M. Schrçder, A novel bismuth-based metal–organic framework for high volumetric methane and carbon dioxide adsorption, *Chem. Eur. J.*, 2014, **20**, 1–7.

61 B. J. Deibert, E. Velasco, W. Liu, S. J. Teat, W. P. Lustig, J. Li, High- performance blue-excitable yellow phosphor obtained from an activated solvochromic bismuth-fluorophore metal−organic framework, *Cryst. Growth Des.*, 2016, **16**, 4178−4182.

62 Y.-J. Kong, L.-J Han, L.-T. Fan, F.-Z. Kong, X. Zhou, A bismuth-based fluorous metal-organic framework for efficient degradation of congo red, *J. Fluor. Chem.*, 2016, **186**, 40-44.

63 M. Albat, N. Stock, Multiparameter high-throughput and in situ X - ray Diffraction study of six new bismuth sulfonatocarboxylates: discovery, phase transformation, and reaction trends, *Inorg. Chem.*, 2018, **57**, 10352–10363.

64 M. Köppen, V. Meyer, J. Ångström, A. K. Inge, N. Stock, Solvent dependent formation of three new Bi-MOFs using a tetracarboxylic acid, *Cryst. Growth Des.*, 2018, **18**, 4060–4067.

65 J. Lu, X.-H. Zhao, B. Bai, F.-K. Zheng, G.-C. Guo, Significant enhancement of cathode-ray scintillation for a conductive Bi-SMOF via in situ partial rare earth ion replacement, *J. Mater. Chem. C*, 2019, **7**, 11099-11103.

66 S. M. F. Vilela, T. Devic, A. Várez, F. Salles, P. Horcajada, A new proton-conducting Bi-carboxylate framework, *Dalton Trans.*, 2019, **48**, 11181-11185.

67 X.-X. Xie, Z.-H. Zhang, J. Zhang, L.-F. Hou, Z.-F. Li, G. Li, Impressive proton conductivities of two highly stable metal−organic frameworks constructed by substituted imidazoledicarboxylates, *Inorg*. *Chem,* 2019, **58**, 5173−5182.

68 R.-L. Liu, L.-L. Zhao, W. Dai, C.-L. Yang, X. Liang, G. Li, A Comparative investigation of proton conductivities for two metal−organic frameworks under water and aqua-ammonia vapors, *Inorg. Chem.*, 2018, **57**, 1474–1482.

69 Z. H. Fard, N. E. Wong, C. D. Malliakas, P. Ramaswamy, J. M. Taylor, K. Otsubo, G. K. H. Shimizu, Superprotonic phase change to a robust phosphonate metal–organic framework, *Chem. Mater.*,2018, **30**, 314–318.

70 Y.-J. Xiao, X.-Y. Guo a, J.-X. Liu, L.-F. Liu, F.-X. Zhang, C. Li, Development of a bismuth-based metal-organic framework for photocatalytic hydrogen production, *Chin. J. Catal.*, 2019, **40**, 1339-1344.

71 Q.-L. Guan, Y.-H. Xing, J. Liu, C. Han, C.-Y. Hou, F.-Y. Bai, Bismuth-carboxylate ligand 1,3,6,8-Tetrakis(*p* - benzoic acid)pyrene frameworks, photophysical properties, biological

imaging, and fluorescent sensor for biothiols, *J. Phys. Chem. C*, 2019, **123**, 23287−23296.

72 P. Lamagni, M. Miola, J. Catalano, M. S. Hvid, M. A. H. Mamakhel, M. Christensen, M. R. Madsen, H. S. Jeppesen, X.-M. Hu, K. Daasbjerg, T. R. Skrydstrup, N. Lock, Restructuring metal–organic frameworks to nanoscale bismuth electrocatalysts for highly active and selective CO_2 reduction to formate, *Adv. Funct. Mater.*, 2020, **30**, 1910408.

73 C. Orellana-Tavra, M. Köppen, A. Li, N. Stock, D. Fairen-Jimenez, Biocompatible, crystalline, and amorphous bismuth-based metal−organic frameworks for drug delivery, *ACS Appl. Mater. Interfaces*, 2020, **12**, 5633−5641.

74 A. C. Wibowo, S. A. Vaughn, M. D. Smith, H. Z Loye, Novel bismuth and lead coordination polymers synthesized with pyridine-2,5-dicarboxylates: two single component "white" light emitting phosphors, *Inorg. Chem.*, 2010, **49**, 11001–11008.

75 A. C. Wibowo, M. D. Smith, H. Z. Loye, Structural diversity of metal-organic materials containing bismuth(III) and pyridine-2,5-dicarboxylate, *Cryst. Growth Des.*, 2011, **11**, 4449–4457.

76 A. C. Wibowo, M. D. Smith, H. Z. Loye, A new Kagome´ lattice coordination polymer based on bismuth and pyridine-2,5-dicarboxylate: structure and photoluminescent properties, *Chem. Commun.*, 2011, **47**, 7371–7373.

77 A. C. Wibowo, M. D. Smith, J. Yeon, P. S. Halasyamani, H. Z. Loye, Novel 3D bismuth-based coordination polymers: synthesis, structure, and second harmonic generation properties, *J. Solid State Chem.*, 2012, **195**, 94–100.

78 A. Thirumurugan, W. Li, A. K. Cheetham, Bismuth 2,6-pyridinedicarboxylates: assembly of molecular units into coordination polymers, CO_2 sorption and photoluminescence, *Dalton Trans.*, 2012, **41**, 4126-4134.

79 S. R. Sushrutha, S. Natarajan, Bismuth carboxylates with brucite and fluorite-related structures: synthesis structure and properties, *Cryst. Growth Des.*, 2013, **13**, 1743–1751.

80 Y.-J. Huang, Y.-Q. Zheng, H.-L. Zhu, J.-J. Wang, Hydrothermal synthesis of bismuth (III) coordination polymer and its transformation to nano α-Bi_2O_3 for photocatalytic degradation, *J. Solid State Chem.*, 2016, **239**, 274–281.

81 L. Kan, J.-T. Li, X.-L. Luo, G.-H. Li, Y.-L. Liu, Three novel bismuth-based coordination polymers: synthesis, structure and luminescent properties, *Inorg. Chem. Commun.*, 2017, **85**, 70–73.

82 R.-Q. Zhang, Y.-Y. Liu, Y. An, Z.-Y. Wang, P. Wang, Z.-K. Zheng, X.-Y. Qin, X.-Y. Zhang, Y. Dai, B.-B. Huang, A water-stable triazine-based metal-organic framework as an efficient adsorbent of Pb (II) Ions, *Colloid Surf. A-Physicochem. Eng. Asp.*, 2019, **560**, 315-322.

83 R.-Q. Zhang, Y.-Y. Liu, Z.-Y. Wang, P. Wang, Z.-K. Zheng, X.-Y. Qin, X.-Y. Zhang, Y. Dai, M. Whangboa, B.-B. Huang, Selective photocatalytic conversion of alcohol to aldehydes by singlet oxygen over Bi-based metal-organic frameworks under UV–vis light irradiation, *Appl. Catal. B-Environ.*, 2019, **254**, 463–470.

84 T. Rhauderwiek, C. D. S. Cunha, H. Terraschke, N. Stock, Bismuth coordination polymers with 2,4,6-pyridine tricarboxylic acid: high-throughput Investigations, crystal structures and luminescence properties, *Eur. J. Inorg. Chem.*, 2018, **27**, 3232-3240.

85 A. K. Adcock, B. Gibbons, J. D. Einkauf, J. A. Bertke, J. F. Rubinson, D. T. D. Lill, K. E. Knope, Bismuth (III) - thiophenedicarboxylates as host frameworks for lanthanide Ions: synthesis, structural characterization, and photoluminescent behavior, *Dalton Trans.*, 2018, **47**, 13419-13433.

86 S. Iram, M. Imran, F. Kanwal, Z. Iqbal, F. Deeba, Q. J. Iqbal, Bismuth (III) based metal organic frameworks: luminescence, gas adsorption, and antibacterial studies, *Z. Anorg. Allg. Chem.*, 2019, **645**, 50-56.

87 A. García-Sánchez, M. Gomez-Mendoza, M. Barawi, I. J. Villar-Garcia, M. Liras, F. Gándara, V. A. D. L. P. O'Shea, Fundamental Insights into photoelectrocatalytic hydrogen production with a hole-transport bismuth metal−organic framework, *J. Am. Chem. Soc.*, 2020, **142**, 318−326.

88 H. Gao, X.-M. Zhang, Three novel Bi(III) complexes with in situ generated anilate ligands: unusual oxidation of cyclohexanedione to dihydroxy benzoquinone, *Dalton Trans.*, 2012, **41**, 1562-1567.

89 S. M. F. Vilela, A. A. Babaryk, R. Jaballi, F. Salles, M. E. G. Mosquera, Z. Elaoud, S. V. Cleuvenbergen, T. Verbiest, P. Horcajada, Novel non-linear optically active bismuth-camphorate coordination polymer, *Eur. J. Inorg. Chem.*, 2018, **20-21**, 2437-2443.

90 A. A. Babaryk, O. R. C. Almengor, M. Cabrero-Antonino, S. Navalón, H. García, P. Horcajada, A semiconducting $Bi_2O_2(C_4O_4)$ coordination polymer showing a photoelectric response, *Inorg. Chem.*, 2020, **59**, 3406−3416.

Inorganic Chemistry Frontiers

View Article Online
DOI: 10.1039/D0QI01055C

Table 1. A summary of the Bi-MOFs that appeared in this review.

MOFs	Synthetic method	Structure	Property	Ref.
$Bi_2O_2(3,5\text{-pdc})_2$	Hydrothermal synthesis	3D	Thermal stability	35
$Bi(O_3SC_2H_4SO_3)_{1.5}(H_2O)_2$	Hydrothermal synthesis	3D	——	36
Bi-mna	Solvothermal synthesis	3D	Photocatalytic	37
$[Bi(BTC)(H_2O)]\cdot 2H_2O\cdot CH_3OH$ (CAU-17)	Microwave synthesis	3D	——	40
Bi(BTB) (CAU-7)	Solvothermal synthesis and microwave synthesis	3D	Organocatalysis	41
$Bi_2(O)(OH)(TATB)$ (CAU-35)	Solvothermal synthesis	3D	——	42
$[Bi(TATB)]\cdot DMF\cdot 6H_2O$ (CAU-7-TATB)	Microwave synthesis	3D	——	42
CAU-7-TATB-NH_2	Microwave synthesis	3D	Post-modified	42
$(H_2Im)[Bi(1,4\text{-bdc})_2]$	Mechanochemical synthesis	3D	——	43
$[Bi(2,5\text{-pdc})(NO_3)_2(H_2O)_2]\cdot H_2O$	Mechanochemical synthesis	1D	——	43
$[Bi(bda)_3]_n$	Reflux method	——	Luminescent	44
[Bi(HBTC)(Ac)	Reflux method	2D	——	45
$[Bi(1,4\text{-bdc})_2(DMF)]\cdot(Hdma)\cdot 2DMF$	Solvothermal synthesis	2D	——	48
$[Bi(1,4\text{-bdc})_2]\cdot(Hdma)\cdot DMF$	Solvothermal synthesis	3D	——	48
$[Bi_4(1,4\text{-bdc})_7(HIm)]\cdot 2(Hdma)\cdot 2DMF$	Solvothermal synthesis	3D	Luminescent	48
$[Bi(1,4\text{-bdc})_2]\cdot(Hdma)$	Solvothermal synthesis	3D	Luminescent	48
$Bi_2(1,4\text{-bdc})_2(dfp)_2]\cdot DMF$	Solvothermal synthesis	1D	Antibacterial activity	49
$[Bi_2(1,4\text{-bdc})(dfp)_4(H_2O)_2]\cdot 2DMF$	Solvothermal synthesis	1D	Antibacterial activity	49
$[Bi_2(1,4\text{-bdc-}NH_2)(dfp)_4(H_2O)_2]\cdot 2DMF$	Solvothermal synthesis	——	Antibacterial activity	49
$[Bi_2\{1,4\text{-bdc-}(OH)_2\}(dfp)_4(H_2O)_2]\cdot 2DMF$	Solvothermal synthesis	——	Antibacterial activity	49
Bi-bdc-ST	Solvothermal synthesis	——	Photocatalytic	50
Bi-bdc-MW	Microwave synthesis	——	Photocatalytic	50
$Bi_2(O)(Pyr)(H_2O)$	Hydrothermal synthesis	2D	Luminescence	51
Bi(HPyr)	Hydrothermal synthesis	3D	Luminescence	51
Bi(HPyr)	Hydrothermal synthesis	3D	Luminescence	51
$Bi(Tri)(H_2O)$	Hydrothermal synthesis	3D	Luminescence	51
Bi(Tri)	Hydrothermal synthesis	——	Luminescence	51
$[(Bi(BTC)(H_2O)]\cdot H_2O$	Hydrothermal synthesis	3D	Luminescence	51
$Bi_6O_5(BTC)_2(HBTC)$	Hydrothermal synthesis	3D	Luminescence	51
$Bi_2(O)(OH)(HBTC)(NO_3)$	Hydrothermal synthesis	3D	Luminescence	51
$[Bi(Pyr)_{0.5}(2,2'\text{-bipy})(NO_3)(DMF)]$	Solvothermal synthesis	1D	Luminescent and catalytic	52
[Bi(IDA)(IDAH)]	Solvothermal synthesis	1D	Luminescent and catalytic	52
$([Bi(BTC)(DMF)]\cdot DMF\cdot 2CH_3OH$	Solvothermal synthesis	3D	Photocatalytic	53
CAU-17	Microwave synthesis	3D	Heterogeneous catalysis	54
CAU-17	Solvothermal synthesis	3D	Selective Capture of SeO_3^{2-}	55
$\{[Bi(BTC)(H_2O)_2]\cdot H_2O\}_n$	Hydrothermal synthesis	3D	Photocatalytic degradation of MO	56
Eu@Bi-MOF, Tb@Bi-MOF and Eu/Tb@Bi-MOF (Bi-MOF, CAU-17)	Solvothermal synthesis	3D	White-light emission and fluorescence sensing	57
$[Bi(BTC)\ (H_2O)]\cdot H_2O$	Hydrothermal synthesis	3D	Detection of $Fe^{3+}$and $Cr_2O_7^{2-}$ ions	58
Bi(BTC)(DMF)	Solvothermal synthesis	2D	Electrocatalytic reduction	59
$[Bi_2(BPTC)_{1.5}(H_2O)_2]\cdot 3.5DMF\cdot 3H_2O$ (NOTT-220-solv)	Solvothermal synthesis	3D	Gas adsorption	60

MOFs	Synthetic method	Structure	Property	Ref.
K[Bi(tcbpe)(DMF)$_2$]·xDMF (LMOF-401)	Solvothermal synthesis	3D	Optical properties	61
[Bi(OOCC$_6$F$_5$)$_3$(2,2'-bipy) (H$_2$O)$_2$] (Bi-FMOFs)	Hydrothermal method	2D	Degradation of Congo red	62
[Bi$_2$(H$_2$TCPB)(TCPB)(H$_2$O)$_2$]·xH$_2$O (CAU-31)	Solvothermal synthesis	3D	Gas adsorption	64
(Hdma)[Bi(TCPB)(H$_2$O)]·xH$_2$O (CAU-32)	Solvothermal synthesis	3D	Gas adsorption	64
[Bi$_4$(O)$_2$(OH)$_2$(H$_2$TCPB)(TCPB)(H$_2$O)$_2$]·xH$_2$O (CAU-33)	Solvothermal synthesis	3D	Gas adsorption	64
[(Hdma)Bi(1,4-ndc)$_2$(DMF)]$_n$·nDMF	Solvothermal synthesis	2D	Photoluminescent and Cathode ray luminescence (CL)	65
Bi$_4$(HAzoBTC)$_2$(AzoBTC)(OH)$_2$(H$_2$O)$_4$]·7H$_2$O (IEF-2)	Hydrothermal method	3D	Proton conduction	66
Bi-TBAPy	Solvothermal synthesis	3D	Photocatalytic hydrogen production	70
Bi(TBAPy)	Solvothermal synthesis	3D	Photoluminescent, biological imaging and fluorescence sensing	71
CAU-7	Solvothermal synthesis	3D	Electrochemical CO_2 reduction reaction (eCO_2RR)	72
CAU-7	Microwave synthesis	3D	Drug delivery systems (DDSs)	73
Bi(2,5-pdc)(2,5-Hpdc)(H$_2$O)	Hydrothermal method	1D	Photoluminescent	75
K$_4$Bi(2,5-pdc)$_3$(2,5-Hpdc)(H$_2$O)$_{3.3}$	Hydrothermal method	2D	——	75
(Hdma)$_3$Bi(2,5-pdc)$_2$(2,5-Hpdc)$_2$	Solvothermal synthesis	1D	——	75
Bi(2,5-pdc)$_2$(H$_3$O$^+$)(H$_2$O)$_{0.83}$	Solvothermal synthesis	2D	Photoluminescent	76
Bi$_2$O$_2$(2,5-pdc)	Hydrothermal method	3D	Second harmonic generation (SHG)	77
Bi$_4$Na$_4$L$_8$(EtOH)$_{3.1}$(H$_2$O)$_{3.4}$	Solvothermal synthesis	3D	Second harmonic generation (SHG)	77
[LiBi(2,6-pdc)$_3$(H$_2$O)]·2(Hdma)	Solvothermal synthesis	1D	Gas adsorption and photoluminescence	78
Li$_5$Bi(2,6-pdc)$_4$(H$_2$O)$_2$	Solvothermal synthesis	3D	Gas adsorption	78
[Bi(HIDC)IDC)]	Hydrothermal method	1D	Heterogeneous Catalytic	79
[Bi(μ$_2$-OH)(3,4-pdc)]	Hydrothermal method	3D	Heterogeneous Catalytic	79
Bi$_2$(2,6-Hpdc)$_2$(2,6-pdc)$_2$·2H$_2$O	Hydrothermal method	1D	Photocatalytic degradation	80
(Hdma)[Bi(3,5-pdc)(bdc)]·2DMF	Solvothermal synthesis	3D	Detection of nitro explosives	81
(Hdma)[Bi(TDC)$_2$]·1.5DMF	Solvothermal synthesis	3D	——	81
[Bi(bda)$_2$H$_2$O]·xGuest	Solvothermal synthesis	2D	——	81
CAU-7-TATB	Solvothermal synthesis	3D	Adsorbent of Pb (II) Ions	82
CAU-7-TATB	Solvothermal synthesis	3D	Selective organic synthesis	83
[Bi(PTC)(H$_2$O)$_2$]	Hydrothermal method	2D	Luminescence	84
(H$_3$O)[Bi$_2$(PTC)(HPTC)$_2$(H$_2$O)$_2$]	Hydrothermal method	2D	Luminescence	84
α-[Bi(PTC)]	Hydrothermal method	3D	——	84
β-[Bi(PTC)]	Hydrothermal method	3D	——	84
Hpy[Bi(TDC)2(H$_2$O)]·1.5H$_2$O	Routine solution synthesis	2D	Photoluminescence	85
[Hpy]$_3$[Bi$_2$(TDC)$_4$(HTDC)H$_2$O)]·0.74H$_2$O	Routine solution synthesis	2D	——	85
(Hpy)$_2$[Bi(TDC)$_2$(HTDC)]·0.36H$_2$O	Routine solution synthesis	2D	——	85
[Bi(HMMTA)$_3$]$_n$	Heating reflux method	——	Fluorescence and antibacterial	86
[Bi(2,6-NDA)$_3$]$_n$	Routine solution synthesis	——	Fluorescence	86
[Bi(DMP)$_3$]$_n$	Routine solution synthesis	——	Fluorescence and antibacterial	86
[Bi(MBA)$_3$]$_n$	Heating reflux method	——	Fluorescence and antibacterial	86
[Bi$_{12}$(DTTDC)$_{24}$]·12(Hdm)·4DMF·2H$_2$O (IEF-5)	Solvothermal synthesis	3D	Photoelectrocatalytic	87

Inorganic Chemistry Frontiers

View Article Online
DOI: 10.1039/D0QI01055C

Bi(III) MOFs: Syntheses, structures and applications

Qing-Xu Wang and Gang Li*

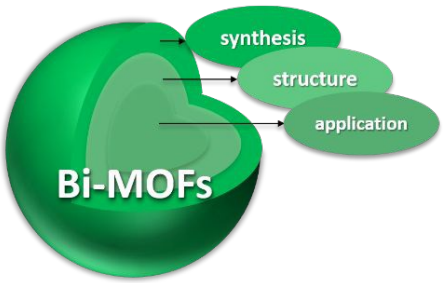

The synthesis methods, structures and applications in catalysis, adsorption, fluorescence, etc. of Bi(III)-based MOFs were reviewed.